AD_____

Award Number: W81XWH-11-1-0256

TITLE: Interrogating Spatio-Mechanical EphA2 Signaling in Cancer

PRINCIPAL INVESTIGATOR: Jay Groves

CONTRACTING ORGANIZATION: The University of California
Berkeley, CA 94704

REPORT DATE: March 2012

TYPE OF REPORT: Annual

PREPARED FOR: U.S. Army Medical Research and Materiel Command
Fort Detrick, Maryland 21702-5012

DISTRIBUTION STATEMENT: Approved for public release; distribution unlimited

REPORT DOCUMENTATION PAGE

Form Approved
OMB No. 0704-0188

1. REPORT DATE *(DD-MM-YYYY)*	2. REPORT TYPE	3. DATES COVERED *(From - To)*
01-03-2012	Annual	1 MAR 2011 - 29 FEB 2012

4. TITLE AND SUBTITLE
Interrogating Spatio-Mechanical EphA2 Signaling in Cancer

5a. CONTRACT NUMBER

5b. GRANT NUMBER
W81XWH-11-1-0256

5c. PROGRAM ELEMENT NUMBER

6. AUTHOR(S)
Jay Groves

E-Mail: jtgroves@lbl.gov

5d. PROJECT NUMBER

5e. TASK NUMBER

5f. WORK UNIT NUMBER

7. PERFORMING ORGANIZATION NAME(S) AND ADDRESS(ES)
The University of California
Berkeley, CA 94704

8. PERFORMING ORGANIZATION REPORT NUMBER

9. SPONSORING / MONITORING AGENCY NAME(S) AND ADDRESS(ES)
U.S. Army Medical Research and Materiel Command
Fort Detrick, Maryland 21702-5012

10. SPONSOR/MONITOR'S ACRONYM(S)

11. SPONSOR/MONITOR'S REPORT NUMBER(S)

12. DISTRIBUTION / AVAILABILITY STATEMENT
Approved for Public Release; Distribution Unlimited

13. SUPPLEMENTARY NOTES

14. ABSTRACT

EphA2 is a receptor tyrosine kinase (RTK) overexpressed in many breast cancers. We have found that upon binding to its native ligand, ephrinA1, EphA2 is reorganized into large-scale clusters. Disrupting this clustering alters downstream signaling events, suggesting that this is a mechanosensitive pathway. Now, our goal is to elucidate how the mechanical properties of a cell and its environment play a role in the EphA2 regulatory system and how this mechanical sensing affects the malignancy of cancer cells. We have found that EphA2 clustering modulates both endocytosis and a PI3K signaling pathway. We have also developed a novel platform for screening small molecule inhibitors that may target other cellular processes, but affect EphA2 phenotypes which, we believe, are important in malignancy. Together, these results provide promising insight into linking the EphA2 mechanosensitive pathway to breast cancer malignancy.

15. SUBJECT TERMS
Mechanosensing, breast cancer, signal transduction, EphA2

16. SECURITY CLASSIFICATION OF:			17. LIMITATION OF ABSTRACT	18. NUMBER OF PAGES	19a. NAME OF RESPONSIBLE PERSON
a. REPORT	b. ABSTRACT	c. THIS PAGE			USAMRMC
U	U	U	UU	46	19b. TELEPHONE NUMBER *(include area code)*

Table of Contents

Introduction

Communication between cells is mediated through cell-surface receptors and the signal transduction reactions they initiate. In recent years, it has become clear that spatial organization of receptors, on length scales from molecular clustering to micron-size pattern formations, plays a key role in the transduction of cellular signals [1-6]. We seek to understand how altered spatial organization of proteins contributes to breast cancer malignancy. Our goal is to understand how mechanical forces, both extra- and intracellular, establish a specific linkage between tissue mechanics, cellular signaling and ultimately, disease. We previously used a fluid supported membrane to present ephrin-A1 to EphA2-expressing human breast cancer cells and observed that EphA2 signaling is sensitive to physical aspects of ligand presentation and, furthermore, that receptor transport is strongly linked to tissue invasion [2]. Based on these observations, we postulate that the functional alteration of the EphA2 receptor in breast cancer has a mechanical component. Thus, the motivating goal of this proposal is to deconstruct the molecular basis for how mechanical forces influence the EphA2 receptor tyrosine kinase signaling cascades in malignant human breast cancer cell lines and then to explore how these forces play a role in cancer progression. In this way, we will examine previously unexplored dimensions of disease mechanism, hopefully contributing insight to better match individual patients with appropriate therapies.

Body

Our central hypothesis is that mechanical properties of a cell and its environment play a role in the EphA2 regulatory system, and that this mechanical sensing affects the malignancy of cancer cells. We chose to pursue three different approaches to probing the mechanical aspects of EphA2 signal transduction: 1) Determining the molecular physiology of the EphA2 mechano-sensing in model human breast cancer cell lines, 2) Using targeted inhibition of signaling molecules involved in EphA2 transport and 3) Examining EphA2 transport in live tissue samples. While this work is still in progress, we have made new discoveries about the physical properties of EphA2 clusters that have led us to several new experiments, described below.

Approach and Previous Data

For all experimental platforms, we display fluorescent, decahistidine-tagged ephrin-A1 on a fluid supported lipid membrane by anchoring the ligand to the membrane using histidine-Ni(II) metal-organic coordination chemistry [7]. This technique allows controllable and quantifiable ligand display coupled with single-cell, high-resolution microscopy capabilities. We cultured live, tumorigenic and invasive EphA2-expressing human breast cancer cells (MDAMB231) on ephrinA1-supported membranes. We previously found that when MDAMB231 cells make contact with ephrinA1 linked to a supported membrane, EphA2 binds to ephrinA1, forming receptor-ligand complexes followed by receptor clustering, phosphorylation and recruitment of the disintegrin and metalloprotease 10 (ADAM10) [2]. We then introduced cells to a supported membrane on a substrate containing grids of nanopatterned chromium diffusion barrier, which redefined the organization of EphA2-ephrinA1 clusters. When MDAMB231 cells contact an ephrinA1-supported membrane with these diffusion barriers, the clustering of EphA2-ephrinA1 is frustrated, and the recruitment of ADAM10 is no longer observed, indicating that downstream signaling is altered by EphA2-ephrinA1 spatial organization.

Results and Progress

Specific Aim 1: Molecular physiology of EphA2 clusters

Developing an assay to probe the molecular physiology of EphA2 clusters

We have developed a novel, monomeric decahistidine ephrinA1 ligand protein, which is a more physiologically relevant compared with the more commonly used pre-dimerized ephrinA1-Fc [8]. Previous studies have shown that soluble, monomeric ephrinA1 will not activate EphA2 on a cell surface, but rather requires preclustered ephrinA1 in solution. We have generated a monomeric ephrinA1 protein which, when bound to a two-dimensional supported lipid membrane, can activate EphA2 in breast cancer cells as measured by receptor degradation via Western blotting (Figure 1). The development of the monomeric ephrinA1 assay allows us to maintain the juxtacrine signaling natural receptor clustering processes, which have been shown to be important signal regulatory mechanisms.

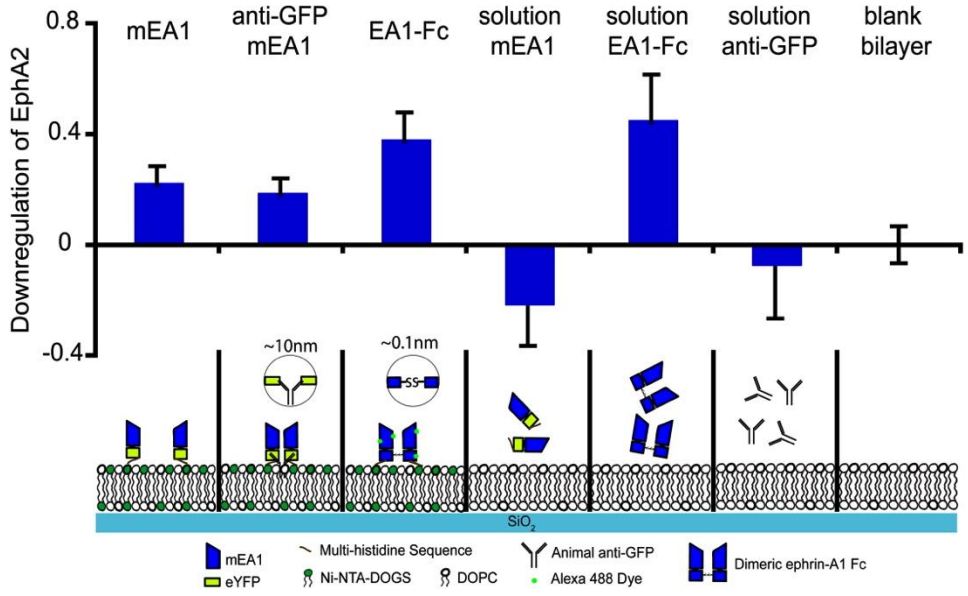

Figure 1. (From Ref 8) Western blots are analyzed from the lysate of MDA-MB-231 cells incubated on different surfaces and in different solutions. The blots are stained for the presence of EphA2. In this case, the degradation of EphA2 is represented by the intensity of an EphA2 band between 75 and 150 kDa. The lower the band intensity, the greater the receptor degradation. Intensity measurements of EphA2 bands are repeated for at least four unique Western blots and the results are averaged across the blots. Soluble mEA1, over a range of concentrations (results not shown), does not induce significant EphA2 degradation, whereas mEA1 on a SLB leads to EphA2 degradation. Antibody cross-linked mEA1 on a SLB leads to EphA2 degradation, although to a lesser degree than pre- clustered EA1-Fc. At low surface densities of mEA1, Western blot analysis is unable to detect significant EphA2 activation.

EGFR and EphA2 Co-clusters

Understanding the physiology of signaling clusters requires an understanding of how their composition modulates cell behavior. During this funding cycle, we have developed a technique that allows presentation of ligand heterodimers to living cells by using DNA hybridization. When MDAMB231 cells were presented with monomeric EGF and ephrinA1 ligand, EGFR was activated as measured by immunofluorescence staining of tyrosine 1173 phosphorylation on the

EGF receptor (Figure 2a). Furthermore, when we heterodimerized the RTK ligands EGF and EphrinA1 using our DNA hybridization strategy and presented these to MDA-MB-231 cells EGFR was not activated (Figure 2b). Representative cells are shown in Figure 2. We suspect that abrogation of signaling is caused by recruitment of tyrosine phosphatases by EphA2 that dephosphorylate the EGFR, although studies are underway to address this hypothesis. This approach offers the ability to modulate signaling by altering the composition signaling clusters, an approach that could yield insight into rational drug design. In particular, we envision our experiments to dissect the molecular physiology of EphA2 clusters into guiding the development of bispecific antibody therapeutics.

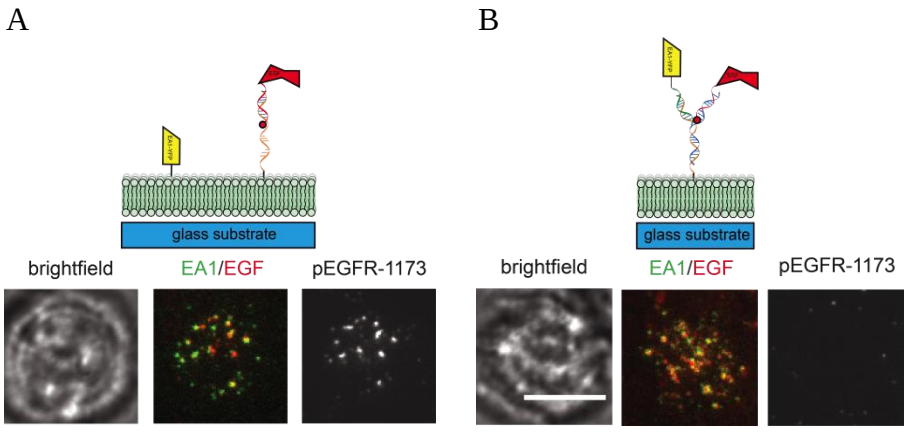

Figure 2. MDAMB231 cells seeded on a supported membrane. A) Presentation of EGF and ephrinA1 that can independently diffuse on the membrane results of clustering of the ligands and activation of EGFR as shown by tyrosine phosphorylation. B) Presentation of a heterodimer of these ligands results also in clustering of the ligands, but not in activation of the EGF receptor.

PI3K Spatial Organization

The development of a more physiologically relevant monomeric ephrinA1 platform allowed us to begin probing the molecular physiology of the EphA2-ephrinA1 clusters. Our targeted proteins are those that colocalize (or antilocalize) with EphA2 and are also known to be misregulated in cancer. Following identification of those proteins, we can then examine the significance of those interactions. Because previous research reports that EphA2 interacts with PI3K upon ephrinA1 binding [9], we began by looking into the PI3K pathway. The PI3K signaling pathway, which promotes cell survival, growth, and proliferation, is known to be abnormally activated in numerous types of human cancers [10], and is one of the most important signaling pathways to target cancer [11]. However, no direct evidence of PI3K activation upon Eph/Ephrin interaction has been observed in live cells. Here, we have monitored PI3K activity and localization during EphA2 activation through live cell labeling of $PI(4,5)P_2$ and $PI(3,4,5)P_3$ with fluorescent PLCd1-PH and Akt-PH biosensors, [12] respectively. Because $PI(4,5)P_2$ and $PI(3,4,5)P_3$ are the reactant and the product of PI3K activation, the spatial organizations of them can reflect PI3K activity. We visualized that $PI(3,4,5)P_3$ (the product of PI3K activity) colocalizes with ephrinA1 while $PI(4,5)P_2$ (the reactant of PI3K activity) antilocalizes with ephrinA1 (Figure 3). This spatial organization of $PI(4,5)P_2$ and $PI(3,4,5)P_3$ at EphA2/EphrinA1 cluster sites illustrates the signaling of PI3K triggered by the activation of EphA2 in live MDAMB231 cells.

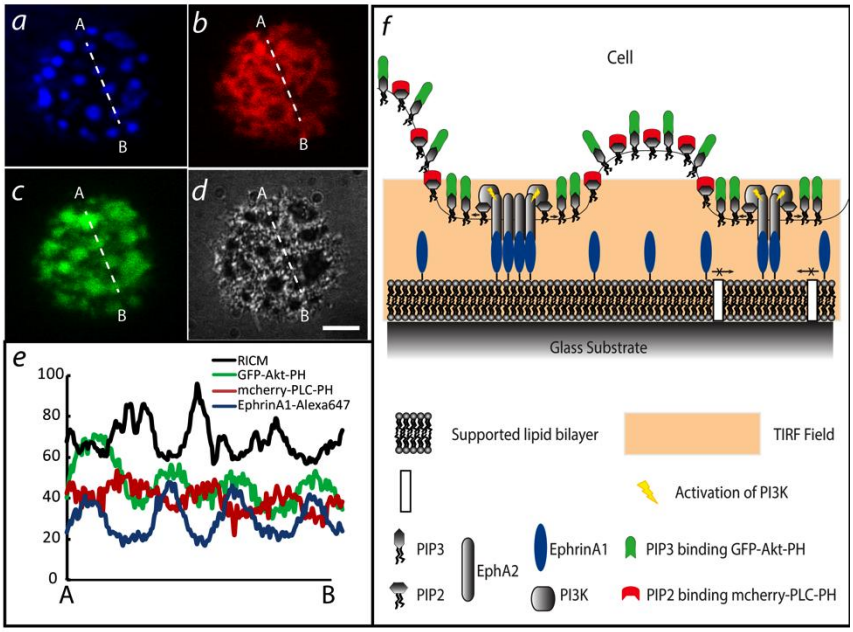

Figure 3. Three-color Total Internal Reflection Fluorescence (TIRF) imaging of MDAMB231 cells on an ephrinA1 supported membrane. A) Supported membrane with ephrinA1 labeled with Alexa Fluor 647, B) cellular PIP2 binding mcherry-PLC-PH, and C) cellular PIP3 binding GFP-Akt-PH. D) topography imaging of the cell/bilayer interface using Reflection interference contrast microscopy (RICM), E) Intensity profiles of each channel along the line AB. F) The schematic illustration of the system: PIP_3, the product of PI3K activation, generates at the cluster sites of EphA2/EphrinA1 and diffuses along the cell membrane; whereas $PI(4,5)P_2$, the reactant of PI3K activation, is excluded from the EphA2/EphrinA1 clusters. Scale bars: 5μm.

Interestingly, when we frustrated ephrinA1 clustering, we did not see a change in this localization trend. The antilocalization of PIP_2 with EphA2/EphrinA1 persists under physical perturbations of EphrinA1 using patterned substrates (Figure 4) indicating that the PI3K activation by ephrinA1 is robust and is not affected by the cluster size.

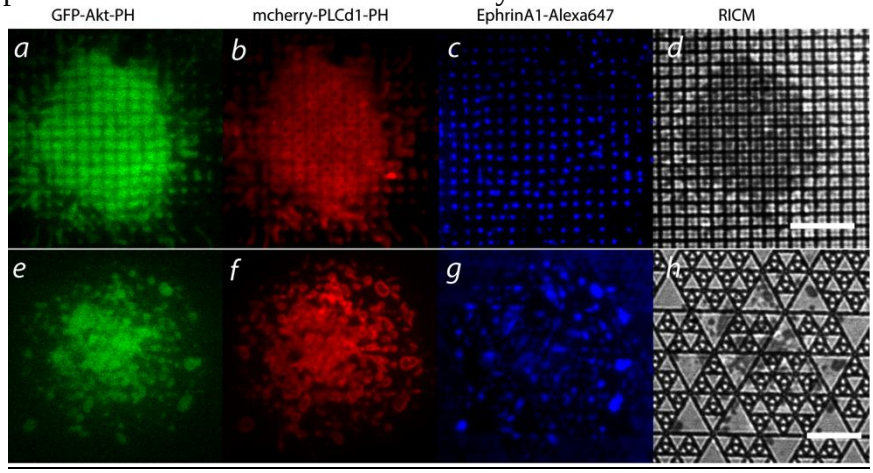

Figure 4. Three-color Total Internal Reflection Fluorescence (TIRF) imaging of MDAMB231 cells on an ephrinA1 supported membrane. A,E) Cellular PIP_3 binding GFP-Akt-PH, B,F) cellular PIP_2 binding mcherry-PLC-PH, and C,G) supported membrane with ephrinA1-A647. D,H) topography imaging of cell/bilayer interface using Reflection interference contrast microscopy (RICM). The first row of images (A-D) was taken on 1μm grids. The protein clusters formed uniformly on the 1μm grids. The images in the second row (E-H) were taken on triangular patterns with mixed sizes, Eph/Ephrin forms different sizes of clusters on triangle patterns. Anti-colocalization of mcherry-PLCd1-PH (PIP_2) and Eph/Ephrin is observed for both patterns. Scale bars: 5μm

EphA2-ephrinA1 Endocytosis

While screening through molecules that constitute the EphA2-ephrinA1 clusters, we found that dynamin2, a large GTPase implicated in the scission of budding endocytic vesicles colocalizes with EphA2-ephrinA1 clusters (Figure 5a). We also found that clathrin, a triskeleton involved in forming coated-pits during vesicle formation, colocalizes with EphA2-ephrinA1 (Figure 5b). These findings led us to investigate if endocytosis of EphA2-ephrinA1 is sensitive to the spatial organization of EphA2-ephrinA1. We developed a robust and novel endocytosis assay to answer this question. EphrinA1 is fluorescently labeled and bound to a supported lipid membrane; MDAMB231 cells are then seeded onto the membrane and allowed to interact with ephrinA1 for 45 minutes. Cells are then fixed and internalized ephrinA1 is imaged using spinning disk confocal microscopy. We then use an automated, high throughput selection process to quantify the amount of internalized ephrinA1 in clusters. Using this assay allows detection of small changes in the amount of internalized ephrinA1.

A

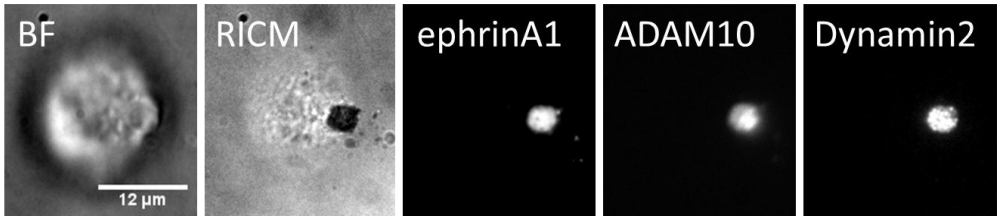

B

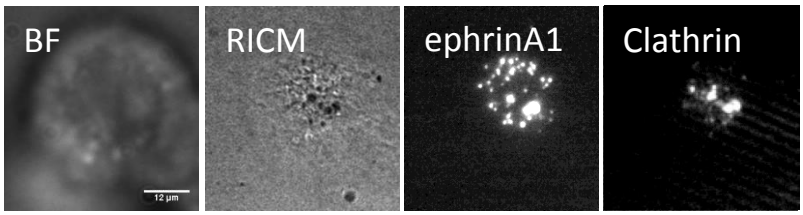

Figure 5. Representative bright field, RICM and epifluorescence images of MDAMB231 cells on an ephrinA1-supported membrane. A) Cells were cultured on a supported membrane displaying ephrinA1-YFP and allowed to cluster ephrinA1 for one hour. BF is a representative bright field image of an MDAMB231 cell. The RICM (reflection interference contrast microscopy) image shows that the region of tightest cell adhesion to the supported membrane corresponds to ephrinA1 recruitment. The three epifluorescence images were taken using Total Internal Reflection Fluorescence (TIRF) microscopy. B) Cells were transfected with a clathrin fluorescent fusion protein and cultured on an ephrinA1-YFP supported membrane for 30 minutes. Images were taken using TIRF microscopy.

To determine the response of endocytosis to physical aspects of ephrinA1 presentation, we used the nanopatterned supported membranes to restrict the size and transport of EphA2-ephrinA1 clusters. The endocytosis assay revealed that physically redefining EphA2-ephrinA1 organization using these patterned membranes alters the internalization of EphA2. Small grid pitches, which effectively decreased the EphA2-ephrinA1 cluster size resulted in decreased amounts of endocytosed EphA2, indicating that endocytosis is modulated by EphA2-ephrinA1 cluster size or transport (Figure 6b). We also found that using Pitstop2, a small-molecule inhibitor of clathrin [13], resulted in a dramatic decrease in the amount of ephrinA1 internalized, indicating that EphA2-ephrinA1 is likely endocytosed via a clathrin-mediated pathway (Figure 6a). Finally, we have found that ADAM10 activity is likely required for the endocytosis of EphA2-ephrinA1. Together, these results suggested that part of the molecular basis of EphA2 mechanosensitivity involves regulation of an endocytic pathway.

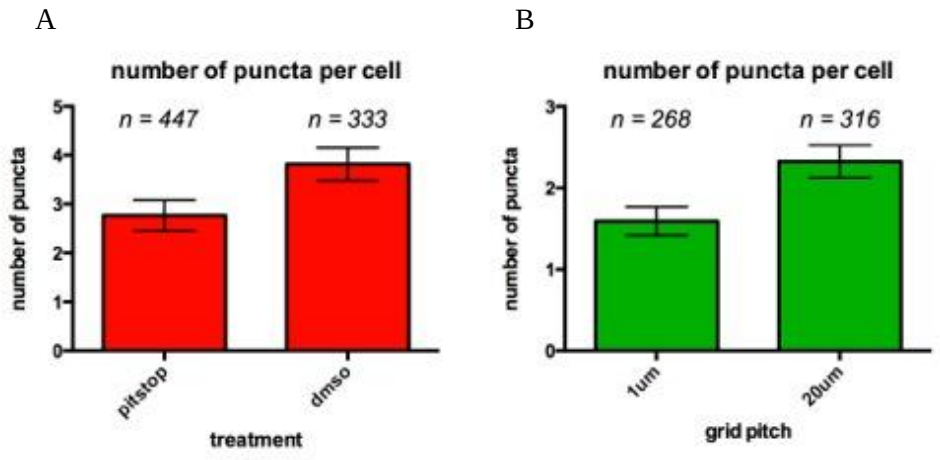

Figure 6. Plots of total internal number of ephrinA1 puncta, which is a readout of the rate of endocytosis of the receptor/ligand pair. A. Number of internal ephrinA1 puncta of cells adhered to an ephrinA1 supported membrane. Cells were treated with the small molecule inhibitor, Pitstop2, or DMSO as a control. B. Number of internal ephrinA1 puncta of cells adhered to an ephrinA1 supported membrane with either 1 μm or 20 μm gridded substrates. $P < 0.05$ for both experiments. The number of cells n is reported for each condition.

Specific Aim 2: Targeted inhibition of signaling molecules involved in EphA2 transport

We have developed a unique experimental platform in which small molecule inhibitors can easily be screened at a single-cell level [manuscript in preparation and appended]. We fabricated nanometer scale ordered arrays of gold [14] nanoparticles embedded within a supported membrane to present different obstacles to the reorganization of EphA2-ephrinA1 clustering. This platform allows three ephrinA1 presentation scenarios: 1) completely mobile ephrinA1 (ephrinA1 is linked to the supported membrane, but nanoparticles are not functionalized), 2) completely immobile ephrinA1 (no ephrinA1 on the supported membrane, but nanoparticles are functionalized with ephrinA1) and 3) a hybrid display of both membrane-bound, fluid ephrinA1 and nanoparticle functionalized, immobile ephrinA1. When using this assay on MDAMB231 cells, we observed that the cells cannot efficiently transport EphA2-ephrinA1 on hybrid-displayed ephrinA1 supported membranes (both mobile and immobile ephrinA1 is presented). When this assay was tested among a panel of breast cancer cell lines, we found that the transport of EphA2 was less affected by the hybrid display of ephrinA1 in cell lines with a lower invasion potential. For instance, MCF10A cells, a noninvasive and non-tumorigenic breast epithelial cell line, can still transport EphA2-ephrinA1 when presented with a hybrid display of ephrinA1 (Figure 7). The transport of EphA2-ephrinA1 on a hybrid display was inversely proportional to the invasiveness and tumorigenicity of the cell line.

We believe the disruption of transport is a symptom of misregulation of another pathway in invasive breast cancer cells and we can now use this platform in conjunction with a high throughput chemical genetic screen using small molecule inhibitors to find these pathways. A drug that rescues transport of EphA2-ephrinA1 clusters on a nanoparticle array will lead us to the broken link in EphA2 regulation in these cell lines and would be a major advance in the effort to

determine the role of EphA2 in breast cancer. Ultimately, these results could provide a drug screening platform for the development of dual-targeted drug therapies

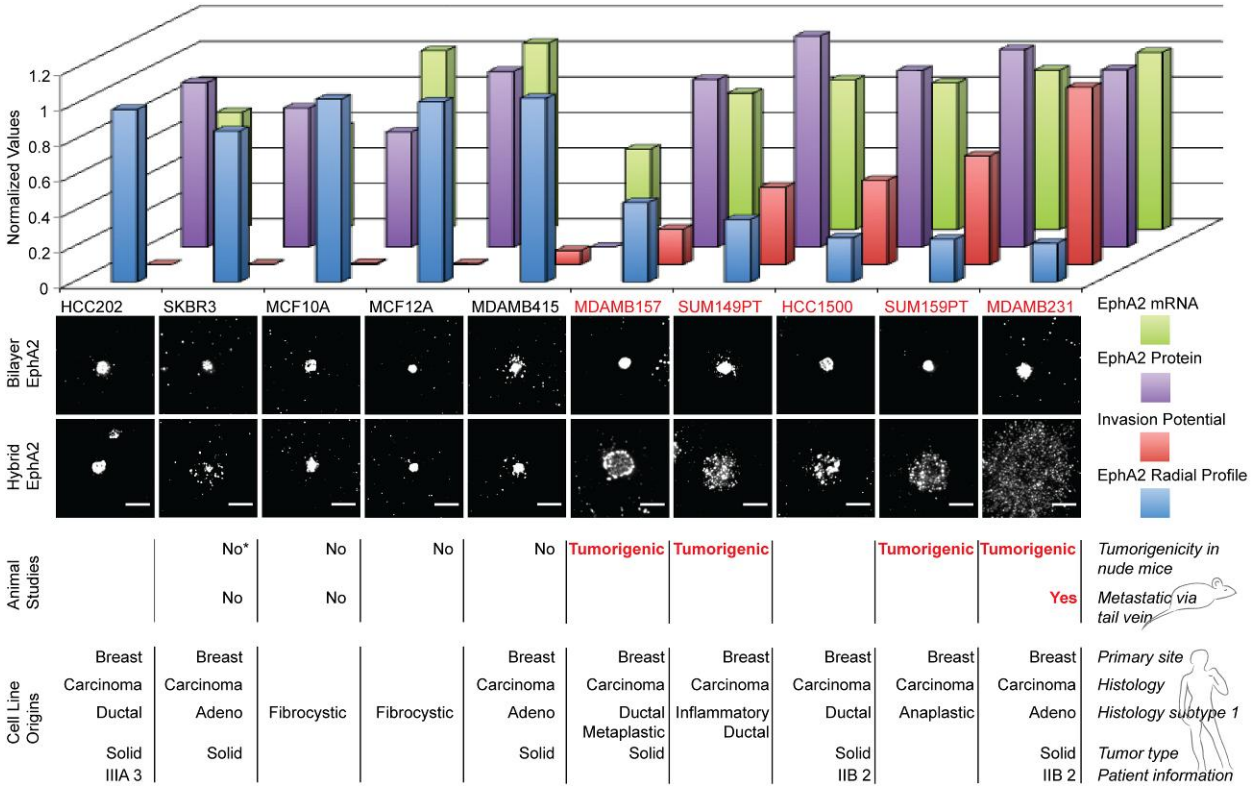

Figure 7 (from appended manuscript). Breast cancer cell line panel study. A panel consisting of 10 human breast cell lines are individually deposited on the hybrid platform. The radial profile of EphA2 was measured for cells that were deposited on the hybrid side and normalized to the radial profile of control cells from the same experiment, on the bilayer only side, to eliminate contributions from staining differences and cell-to-cell variations in EphA2 expression. For all cell lines, on the glass side displaying only mobile EA1, EphA2 is centrally transported. This is consistent with previous reports.[20] For the cell lines on the nanoparticle side displaying the hybrid presentation, this situation changes dramatically; instead of forming a central domain, EphA2 clusters are distributed over the cell – substrate contact area as the respective invasion potential values increase. Invasion potential values, EphA2 protein expression levels, EphA2 mRNA levels (plotted as $\log_2$), and cell line origins were taken from published sources.[19, 28, 34] The animal studies of tumorigenicity and metastasis, correlates with the EphA2 radial profile and invasion potentials, and were taken from published sources.[35-42] The cell line SKBR3 was found to be tumorigenic in one report (*).[43] A total of 200 cells were selected and analyzed. Scale bar are all 10μm.

Specific Aim 3: Examining EphA2 transport and associated molecular physiology in vivo

Our expanded effort in aims one and two have led us to follow up on our serendipitous discoveries using the nanoparticle array assay. We now have access to human breast cancer surgery samples, which, we believe, will provide us with a unique resource to directly compare our human cancer cell line discoveries to live primary cancer cell samples. Much information regarding invasiveness, tumorigenicity, and malignancy of breast cancer cell lines has previously

been determined in mouse model systems. While using an established mouse model system has the potential to provide some insights, we believe our findings will have a more direct impact on understanding the molecular basis of EphA2 mechanosensing and its impact in cancer invasion, malignancy, and ultimate patient prognosis by studying primary human cancer cell samples. We have recently been given a unique opportunity to work directly with pathologists and cancer cell biologists at the University of California San Francisco, so we are evaluating our animal studies to determine if we will gain more insight following this other direction. **We have not yet begun animal sample studies under this funded program.**

Key Research Accomplishments

- Development of a monomeric histidine-tagged ephrinA1 protein for membrane-bound ephrinA1 stimulation of EphA2 in live cancer cells
- Determining that EGFR, endocytosis and PI3K play key roles in regulating the molecular physiology of EphA2 clusters
- Development of a live-cell small molecule inhibitor screening assay

Reportable Outcomes

Manuscripts

- Xu, Q. et al., EphA2 Receptor Activation by Monomeric Ephrin-A1 on Supported Membranes. Biophyscial J., 2011 **101**(11): p. 2731-39.
    - Seed support for biomedical aspects of this work was provided by this grant and acknowledged in this manuscript
- Lohmüller, T. et al., EphA2-ephrin-A1 Transport is Frustrated by Nanoscale Obstacle Arrays, but only in Invasive Cancer Cell Lines, manuscript in preparation and appended.

Presentations

- "EphA2-EphrinA1 signaling and PI(4,5)P2 spatial organization on breast cancer cells." Aiwei Tian (Poster), 56th Biophysical Society meeting, February 2012, San Diego, CA
- "Determining if spatio-mechanosensitivity of EphA2 signaling stems from physical impedance of endocytosis." Adrienne Greene, (Poster), 56th Biophysical Society meeting, February 2012, San Diego, CA
- "Spatial organization of Eph2 and its effects on internalization and signaling in living cells." Samuel Lord (Poster), 56th Biophysical Society meeting, February 2012, San Diego, CA
- "Determining if spatio-mechanosensitivity of EphA2 signaling stems from physical impedance of endocytosis." Adrienne C. Greene (Poster), Systems Imaging: Applications in Immunology and Cencer meeting, January 2012, University of New Mexico Cancer Center, NM. Also presented at American Society for Cell Biology meeting, December 2011, Denver, CO

- "EphA2 Spatial Organization and Mechanobiology in Breast Cancer Cells on Supported Lipid Bilayers." Samuel Lord (Poster), DoD Breast Cancer Research Program Era of Hope 2011 Conference, August 2011, Orlando, FL
- "Hybrid Static/Fluid Synthetic Substrates to Investigate the Cell-Cell Interface." Theobald Lohnueller (Poster), 2011 Physical Sciences Oncology Center site visit, August, 2011, Berkeley, CA
- "Elucidating the role of ADAM10 during EphA2 endocytosis." I. Jeena Lee (Poster), 2011 Physical Sciences Oncology Center site visit, Berkeley, CA, August, 2011
- "Spatial Organization and the Mechanics of Signal Transduction in Cell Membranes." Samuel Lord (Oral Presentation), Conference on Biological Membranes and Membrane Proteins, June 2011, Snowmass, CO

Degrees Obtained

- Qian Xu, PhD

Funding Applied for Based on Work Supported by this Grant

- Adrienne C. Greene: Department of Defense, National Defense Science and Engineerng Graduate (NDSEG) Fellowship (2011)

Employment or Research Opportunities Applied for and/or Received Based on Experience/Training Supported by this Award

- Theobald Lohmüller: Nanochemistry Group Leader, Chair for Photonics and Optoelectronics, Ludwig-Maximilians-Universität München
- Dr. Qian Xu: Postdoctoral Research in Professor Taekjip Ha's laboratory

Conclusions

Here we report significant progress on understanding the role of EphA2 mechanosensing in cancer malignancy. We have unraveled that three important mechanisms involved in the EphA2-ephrinA1 mechanosensitivity include EGFR signaling, endocytosis and the PI3K pathway. To the best of our knowledge, misregulation of these two pathways have not been implicated in mechanosensing and breast cancer. To move forward with this work, live cell assays will provide real-time information on the regulation of EphA2 cluster formation. We have also developed a robust live-cell EphA2-clustering assay that identifies clustering phenotypes that correlate to the invasion potential of breast cancer cell lines. We look forward to using this platform to screen for known small molecule inhibitors targeting other signaling pathways that alter the observed EphA2 phenotype. This assay can be exploited as a tool to understand the molecular signaling crosstalk of EphA2 with other signaling pathways, yielding insight into targeted drug design, effective use of existing drugs as well as the regulation of EphA2. Overall, dissecting the EphA2 mechanosensing pathway in breast cancer has yielded promising and influential results. Future work based on these results will clarify the role of EphA2 in breast cancer and how it can be targeted to cure this disease.

References

1. Manz, B.N. and J.T. Groves, *Spatial organization and signal transduction at intercellular junctions.* Nat Rev Mol Cell Biol., 2010. **11**(5): p. 342-52.
2. Salaita, K., et al., *Restriction of Receptor Movement Alters Cellular Response: Physical Force Sensing by EphA2.* Science, 2010. **327**(5971): p. 1380-1385.
3. Mossman, K.D., et al., *Altered TCR signaling from geometrically repatterned immunological synapses.* Science, 2005. **310**(5751): p. 1191-1193.
4. Davis, S., et al., *Ligands for Eph-Related Receptor Tyrosine Kinases That Require Membrane Attachment or Clustering for Activity.* Science, 1994. **266**(5186): p. 816-819.
5. Harding, A.S. and J.F. Hancock, *Using plasma membrane nanoclusters to build better signaling circuits* Trends in Cell Biology, 2008. **18**(8): p. 364-371.
6. Groves, J.T. and M.L. Dustin, *Supported planar bilayers in studies on immune cell adhesion and communication.* Journal of Immunological Methods, 2003. **278**(1-2): p. 19-32.
7. Nye, J.A. and J.T. Groves, *Kinetic Control of Histidine-Tagged Protein Surface Density on Supported Lipid Bilayers.* Langmuir, 2008. **24**(8): p. 4145-4149.
8. Xu, Q. et al., *EphA2 Receptor Activation by Monomeric Ephrin-A1 on Supported Membranes*. Biophycial J, 2011. **101**(11): p. 2731-39.
9. Pandey, A., et al., *Activation of the Eck receptor protein tyrosine kinase stimulates phosphatidylinositol 3-kinase activity.* The Journal of Biological Chemistry, 1994. **269**: 30154-57
10. Samuels, Y. et al., *High frequency of mutations of the PIK3CA gene in human cancers.* Science, 2004. **304**: p 554.
11. Courtney, K.D., et al., *The PI3K pathway as a drug target in human cancer*. Journal of Clinical Oncology, 2010. **28**: 1075-83.
12. Varnai, P. and Balla, T. *Live cell imaging of phosphoinositides with expressed inositide binding protein domains*. Methods, 2008. **46**: 167-76.
13. Kleist, v.L. et al., *Role of the clathrin terminal domain in regulating coated pit dynamics revealed by small molecule inhibition*. Cell, 2011. **146**:p. 471–484.
14. Lohmüller, T. et al., *Supported Membranes Embedded with Fixed Arrays of Gold Nanoparticles.* Nano Lett. 2011. **11**(11): p 4912-8.

Appendices

BIOGRAPHICAL SKETCH

Provide the following information for the Senior/key personnel and other significant contributors in the order listed on Form Page 2.
Follow this format for each person. **DO NOT EXCEED FOUR PAGES.**

NAME	POSITION TITLE
Jay T. Groves	Professor of Chemistry HHMI Investigator
eRA COMMONS USER NAME (credential, e.g., agency login) jaygroves	

EDUCATION/TRAINING *(Begin with baccalaureate or other initial professional education, such as nursing, include postdoctoral training and residency training if applicable.)*

INSTITUTION AND LOCATION	DEGREE *(if applicable)*	MM/YY	FIELD OF STUDY
Tufts University	B.S.	1992	Physics & Chemistry
Stanford University	Ph.D.	1998	Biophysics

A. Personal Statement

I have had a long-standing interest in the physical and biological aspects of cell membranes and have devoted my career to bridging the divide between physical and biological sciences. My group combines aspects of cellular biophysics, physical chemistry, and materials science to study key aspects of signal transduction processes in cell membranes. By this point, my group is intrinsically hybrid, and producing a generation of students who speak the languages of both physical and biological science as native speakers.

B. Positions, Honors, Service and Patents.

Positions and Employment

1998 – 1999 Visiting Scholar, Academia Sinica, Taipei, Taiwan
1999 – 2001 Division Director's Fellow, Lawrence Berkeley National Laboratory, Berkeley, CA
2001 – 2007 Assistant Professor, Dept. Chemistry, University of California, Berkeley, CA
2001 – Faculty Scientist, Lawrence Berkeley National Laboratory, Berkeley, CA
2007 – 2010 Associate Professor, Dept. Chemistry, University of California, Berkeley, CA
2008 – Howard Hughes Medical Institute Investigator
2010 -- Professor, Dept. Chemistry, University of California, Berkeley, CA

Honors and Awards

N. Hobbs Knight Prize Scholarship in Physics, Tufts University (1991)
Highest Honors in Thesis, Tufts University (1992)
Amos Emerson Dolbear Scholarship for Physics, Tufts University (1992)
Elected Phi Beta Kappa, Tufts University (1992)
Merrill Lynch Innovation Grants Forum Entrepreneurship Award (1998)
Burroughs Wellcome Career Award in the Biomedical Sciences (2000)
Searle Scholars Award (2002)
MIT TR100 (2003)
Hellman Family Faculty Award (2004)
Beckman Young Investigator Award (2004)
NSF CAREER Award (2005)
ACS Langmuir Lecture Award (2005)
LBNL Award for Excellence in Technology Transfer (2007)
Nature Biotechnology Award for Outstanding Research Achievement (2008)
University Lecture, Cornell University (2011)

Service

Guest Editor, Langmuir, Special Issue on the Biomolecular Interface, March 2004
Co-Organizer, QB3 Symposium on Cell Membrane Systems and Technology, May 2005

Co-Organizer, MRS Spring Meeting, Mechanotransduction and Engineered Cell-Surface Interactions Symposium, April 17 - 21, 2006, San Francisco, CA
Guest Editor, Materials Research Bulletin, Materials Sci. of Supported Lipid Membranes, July 2006
Guest Editor, J. Struct. Biol., Special Issue on Supported Membranes, October 2009
Editorial Board, Current Opinion in Chemical Biology, 2006 –
Associate Editor, Annual Review of Physical Chemistry, 2006 –

Patents

US 6,699,719 “Biosensor arrays and methods” (Issued March 2, 2004)
US 6,228,326 “Arrays of independently-addressable supported fluid bilayer membranes and methods of use thereof” (Issued May 8, 2001)

C. Selected peer-reviewed publications

46. Science 2005, 310, 1191-1193: “Altered TCR signaling from geometrically repatterned immunological synapses”, Kaspar D. Mossman, Gabriele Campi, Jay T. Groves and Michael L. Dustin. PMID: 16293763
47. Anal. Chem. 2006, 78, 174-180: "Surface binding affinity measurements from order transitions of lipid membrane-coated colloidal particles", Esther M. Winter, and Jay T. Groves. PMID: 16383325
48. ChemBioChem 2006, 7, 436-440: "A Fluid Membrane-Based Soluble Ligand Display System for Live Cell Assays", Jwa-Min Nam, Pradeep M. Nair, Richard M. Neve, Joe W. Gray, and Jay T. Groves. PMC: 2733875
49. Phys. Rev. Lett. 2006, 96, 118101: "Hydrodynamic damping of membrane thermal fluctuations near surfaces imaged by fluorescence interference microscopy", Yoshihisa Kaizuka and Jay T. Groves. PMID: 16605875
50. J. Phys. Chem. B 2006, 110, 8513-8516: "Coupled membrane fluctuations and protein mobility in supported inter-membrane junctions", Raghuveer Parthasarathy and Jay T. Groves. PMID: 16623539
51. Langmuir, 2006, 22, 5095-5099: “Curvature modulated phase separation in lipid bilayer membranes", Raghuveer Parthasarathy and Jay T. Groves. PMID: 16700599
52. Langmuir, 2006, 22, 12, 5384-5384: “Nonequilibrium patterns of cholesterol-rich chemical heterogeneities within single fluid supported phospholipids bilayer membranes”, Annapoorna R. Sapuri-Butti, Qijian Li, Jay T. Groves, and Atul N. Parikh. PMID: 16732666
53. Curr. Op. Chem. Biol., 2006, 10, 544-550: “Spatial mutation of the T cell immunological synapse”, Jay T. Groves. PMID: 17070724
54. J. Am. Chem. Soc., 2006, 128, 15221-15227: “Lipid lateral mobility and membrane phase structure modulation by protein binding”, Martin B. Forstner, Chanel K. Lee, Atul N. Parikh, and Jay T. Groves. PMID: 17117874
55. Science, 2006, 313, 1901-1902: “Unveiling the membrane domains”, Jay T. Groves. PMID: 17008517
56. Biophys. J., 2006, 91, 3600-3606: “Analysis of shape, fluctuations, and dynamics in intermembrane junctions”, Lawrence C.-L. Lin, Jay T. Groves, and Frank L. H. Brown. PMC: 1630473
57. J. Am. Chem. Soc., 2006, 128, 15354-25355: “Control of antigen presentation with a photoreleasable agonist peptide”, Andrew L. DeMond and Jay T. Groves. PMID: 17131984
58. Soft Matt., 2007, 1, 24-33: “Curvature and spatial organization in biological membranes”, Raghuveer Parthasarathy and Jay T. Groves. PMID: PMC Journal – In Process
59. Chem. Soc. Rev., 2007, 35, 46-54: “Micropatterned supported membranes as tools for quantitative studies of the immunological synapse”, Kaspar Mossman and Jay T. Groves. PMID: PMC Journal – In Process
60. Langmuir, 2007, 23, 4, 2052-2057: “Hybrid protein-lipid patterns from aluminum templates”, Bryan L. Jackson and Jay T. Groves. PMID: 17279694
61. Nature Prot. 2007, 2, 1438 - 1444: "Detection of proteins using a colorimetric bio-barcode assay", Jwa-Min Nam, Kyung-Jin Jang, and Jay T. Groves. PMID: 17545980
62. J. Am. Chem. Soc. 2007, 129, 5462 - 5471: "Hierarchical assembly of model cell surfaces: Synthesis of mucin mimetic polymers and their display on supported bilayers", David Rabuka, Raghuveer Parthasarathy, Goo Soo Lee, Xing Chen, Jay T. Groves, and Carolyn R. Bertozzi. PMC: 2535821
63. Annu. Rev. Phys. Chem. 2007, 58, 697 - 717: "Bending mechanics and molecular organization in biological membranes", Jay T. Groves. PMID: 17430092
64. J. Am. Chem. Soc. 2007, 129, 11543-11550: "Synthetic analogues of glycosylphosphatidylinositol

anchored proteins and their behavior in supported lipid bilayers", Margot G. Paulick, Amber R. Wise, Martin B. Forstner, Jay T. Groves, and Carolyn R. Bertozzi. PMID: 17715922
65. J. Phys. Chem. B 2007, 111, 12133-12135: "Molecular orientation of membrane-anchored mucin glycoprotein mimics", Raghuveer Parthasarathy, David Rabuka, Carolyn R. Bertozzi, and Jay T. Groves. PMID: 17915910
66. Proc. Natl. Acad. Sci. USA, 2007, 104, 51, 20332 - 20337: "A chemical approach to unraveling the biological function of the glycosylphosphatidylinositol anchor", Margot G. Paulick, Martin B. Forstner, Jay T. Groves and Carolyn R. Bertozzi. PMC: 2154431
67. Current Opinion in Immunology, 2007, 19, 6, 722 - 727: "Interrogating the T cell synapse with patterned surfaces and photoactivated proteins", Andrew L. DeMond and Jay T. Groves. PMID: 17703931
68. Biophys. J. 2008, 94, 3286-3292: “T cell receptor microcluster transport through molecular mazes reveals mechanism of translocation”, Andrew L. DeMond, Kaspar D. Mossman, Toby Starr, Michael L. Dustin, and Jay T. Groves. PMC: 2275686
69. Langmuir, 2008, 24, 8, 4145 - 4149: "Kinetic control of histidine-tagged protein surface density on supported lipid bilayers", Jeffrey A. Nye and Jay T. Groves. PMID: 18303929
70. J. Am. Chem. Soc., 2008, 130, 18, 5947-5953: "Non-covalent cell surface engineering: incorporation of bioactive synthetic glycopolymers into cellular membranes", David Rabuka, Martin B. Forstner, Jay T. Groves and Carolyn R. Bertozzi. PMC: 2724873
71. Langmuir, 2008, 24, 10, 6189-6193: "Electrical manipulation of supported lipid membranes by embedded electrodes", Bryan L. Jackson, Jeffrey A. Nye and Jay T. Groves. PMID: 18491927
72. Nat. Struct. Mol. Biol., 2008, 15, 452-461: "Membrane-dependent signal integration by the Ras activator Son of sevenless", Jodi Gureasko, William J. Galush, Sean Boykevisch, Holger Sondermann, Dafna Bar-Sagi, Jay T. Groves and John Kuriyan. PMC: 2440660
73. Biophys. J., 2008, 95, 2512-2519: "Quantitative fluorescence microscopy using supported lipid bilayer standards", William J. Galush, Jeffrey A. Nye and Jay T. Groves. PMC: 2517038
74. Annu. Rev. Biomed. Eng., 2008, 10, 311-338: "Fluorescence Imaging of Membrane Dynamics", Jay T. Groves, Raghuveer Parthasarathy, Martin B. Forstner. PMID: 18429702
75. Nat. Biotech., 2008, 26, 7, 825-830: "Electrostatic readout of DNA microarrays with charged microspheres", Nathan G. Clack, Khalid Salaita and Jay T. Groves. PMID: 18587384
76. ChemPhysChem,2008, 9, 12, 1688-1692: "Discrete Arrays of Liquid Crystal-Supported Proteolipid Monolayers as Phantom Cell Surfaces", Amber R. Wise, Jeffrey A. Nye, Jay T. Groves. PMCID: 18651693
77. Soft Matter,2009, 5, 1931-1936: "Like-charge interactions between colloidal particles are asymmetric with respect to sign", Esther W. Gomez, Nathan G. Clack, Hung-Jen Wu and Jay T. Groves. PMID: PMC Journal – In Process
78. Langmuir,2009, 25, 6, 3713-3717: "Effect of support corrugation on silica xerogel-supported phase separated lipid bilayers", Emel I. Goksu, Barbara A. Nellis, Wan-Chen Lin, Joe H. Satcher, Jr., Jay T. Groves, Subhash H. Risbud, Marjorie L. Longo. PMID: 19209917
79. Nano Lett, 2009, 5, 2077-2082: "A nanocube plasmonic sensor for molecular binding on membrane surfaces", William J. Galush, Sarah A. Shelby, Martin J. Mulvihill, Andrea Tao, Peidong Yang, Jay T. Groves. PMID: 19385625
80. Proc. Natl. Acad. Sci. USA, 2009, 106, 31, 12729-12734: “Cluster size regulates protein sorting in the immunological synapse”, Niña C. Hartman, Jeffrey A. Nye, Jay T. Groves. PMC: 2722343
81. J. Struct. Biol. 2009, 168, 1-2: “Supported membranes in structural biology”, Lukas K. Tamm and Jay T. Groves. PMID: 19628042
82. Nat. Chem. Biol. 2009, 5, 11, 783-784: “Physical chemistry of membrane curvature”, Jay T. Groves. PMID: 19841625
83. Nat. Immunol. 2010, 11, 1, 90-96: “TCR and LAT occur in separate domains on T cell membranes, which concatenate during activation”, Björn F. Lillemeier, Manuel A. Mörtelmaier, Martin B. Forstner, Johannes B. Huppa, Jay T. Groves, Mark M. Davis. PMID: 20010844
84. Science 2010, 327, 1380: “Restriction of receptor movement alters cellular response: Physical force sensing by EphA2”, Khalid Salaita, Pradeep M. Nair, Rebecca S. Petit, Richard M. Neve, Debopriya Das, Joe W. Gray, and Jay T. Groves. PMC: 2895569
85. Nat. Rev. Mol. Cell Biol. 2010, 11(5), 342-352: “Spatial organization and signal transduction at intercellular junctions”, Boryana N. Manz and Jay T. Groves. PMID: 20354536

86. Nat. Struct. Mol. Biol., 2010, 17, 659-665: "Molecular mechanisms in signal transduction at the membrane", Jay T. Groves and John Kuriyan. PMID: 20495561
87. PLoS ONE, 2010, 5(7): e11878. doi:10.1371/journal.pone.0011878, "Altered Actin Centripetal Retrograde Flow in Physically Restricted Immunological Synapses.", Cheng-han Yu, Hung-Jen Wu, Yoshihisa Kaizuka, Ronald D. Vale, Jay T. Groves. PMC: 2912367
88. New J. Phys., 2010, 12, 095001, "Bending-mediated superstructural organizations in phase-separated lipid membranes", Yoshihisa Kaizuka, Jay T. Groves. PMID: In Process
89. Med. Biol. Eng. Comput., 2010, 48(10): "Engineering supported membranes for cell biology", Cheng-Han Yu, Jay T. Groves. PMC: 2944960
90. Proc. Natl. Acad. Sci. USA, 2010, 107(45): "Engineering of a synthetic electron conduit in living cells", M. Jensen, Aaron E Albers, Konstantin R. Malley, Yuri Y. Londer, Bruce E. Cohen, Brett A. Helms, Peter Weigele, Jay T. Groves, Caroline M. Ajo-Franklin. PMC: 2984186
91. Communicative & Integrative Biology, 2010, 3:5, 454-457: "Roles of the cytoskeleton in regulating EphA2 signals", Khalid Salaita and Jay T. Groves. PMC: 2974079
92. Current Protocols in Chemical Biology, 2010, 2, 235-269: "Supported Membrane Formation, Characterization, Functionalization, and Patterning for Application in Biological Sciences and Technology", Wan-Chen Lin, Cheng-Han Yu, Sara Triffo, Jay T. Groves.
93. J. Phys. Chem A, 2011, 115(16), 3867-3875: Patterned Two-Photon Photoactivation Illuminates Spatial Regoranization in Live Cells", Adam W. Smith, Alexander A. Smoligovets, Jay T. Groves.
94. Nat. Protoc., 2011, 6, 523-539: "Using patterned supported lipid membranes to investigate the role of receptor organization in intercellular signaling", Pradeep M. Nair, Khalid Salaita, Rebecca S. Petit, Jay T. Groves.
95. PNAS, 2011, 108(22), 9089-909: "T-cell triggering thresholds are modulated by the number of antigen within individual T-cell receptor clusters", Boryana N. Manz, Bryan L. Jackson, Rebecca S. Petit, Michael L. Dustin, Jay T. Groves. PMC: 3107331
96. Curr. Opin. Cell Biol. 2011, 23(4), 370-376: "Signaling clusters in the cell membrane", Niña C. Hartman, Jay T. Groves.
97. Cell, 2011, 146(5), 732-745: "A Mechanism for Tunable Autoinhibition in the Structure of a Human Ca2+/Calmodulin- Dependent Kinase II Holoenzyme", Luke H. Chao, Margaret M. Stratton, Il-Hyung Lee, Oren S. Rosenberg, Joshua Levitz, Daniel J. Mandell, Tanja Kortemme, Jay T. Groves, Howard Schulman, John Kuriyan.
98. Nano Lett, 2011, "Supported Membranes Embedded with Fixed Arrays of Gold Nanoparticles", Theobald Lohmüller, Sara Triffo, Geoff P. O'Donoghue, Qian Xu, Michael P. Coyle, Jay T. Groves.

D. Research Support (in order of relevance to proposed research)

Ongoing Research Support

- KC0304 Groves (PI) 10/1/01-9/30/14
  Department of Energy, SNSET Program, Shared Grant; "Engineering Interactive Biological/Material Interfaces with Nanotechnology"; Goals: Form functional interfaces between living and non-living for energy harvesting and materials fabrication applications.
- HHMI Groves (PI) 9/1/08-8/31/13
  Howard Hughes Medical Institutions Investigator; Goal: General support.
- U54 CA143836 Groves (Co-PI) 8/1/09 – 7/31/14
  Physical Science – Oncology Center; National Cancer Institute, NIH; Goal: Study mechanical aspects of cancer biology at the molecular level.
- BC102681 Groves (PI) 3/1/11-2/28/12
  Department of Defense, Congressionally Directed Medical Research Program: Interrogating Spatio-Mechanical EohA2 Signaling in Cancer.
- 1 PO1 AI091580 Groves (co-PI) 7/15/11-6/30/15
  Deconstructing the Reconstructing the T Cell Signaling Network.

Completed Research Support

- 1000849 Groves (PI) 9/1/00-8/31/05
  Burroughs Wellcome Career Award in the Biomedical Sciences; "Studies of Cell Recognition and Signaling with Micropatterned Lipid Membranes". The major goal of this project was the micro fabrication technology development for studies of living cells.
- 1 R01 GM 64900-01 Groves (PI) 2/1/02-2/28/07
  National Institutes of Health/NIGMS; "Quantitative studies of the immunological synapse"; Overall Goals of Project: Role of spatial organization in T cell receptor signaling.
- 02-C-101 Groves (PI) 7/1/02 – 6/30/06
  The Chicago Community Trust, Searle Scholars Award; "Physical Paradigms of Cell Communication at an Inter-Membrane Synapse"; The major goal of this project is the development and implementation of supported membrane based technology to study cell-cell interactions. Neuronal synapses are used as the test system.
- 002865-UCB Groves (Co-PI) 8/1/02-7/31/07
  NSF/UC Davis, Center for Biophotonics Science and Technology; "Label-Free Bioanalytical Detection On Membrane Surfaces"; Goal: Investigation of label free assays for bioanalytical detection.
- 018335 Groves (PI) 9/1/04 – 8/31/07
  Arnold and Mabel Beckman Foundation; "Dissecting Molecular Mechanisms of Signal Transduction at Cell – Cell Synapses"; This study investigates the advanced micro- and nano-fabrication technology development to examine molecular interactions at cell-cell junctions.
- MCB-0448614 Groves (PI) 7/1/05-6/30/10
  NSF Career; "Mechanisms of Spatial Pattern Formation and Signal Transduction at Intercellular Junctions"; Goal: Imaging and spectroscopy of molecular organization in T cell immunological synapse.
- W81XWH-08-1-0677 Groves (PI) 9/1/08-8/31/10
  US Army Medical Research Acquisition Activity; "Elucidating Metastatic Behavior Through Nanopatterned Membranes"
- KC0203010 Groves (Co-PI)
  Department of Energy, Biomolecular Materials; Goal: Template soft matter assembly.

Rev. 11/29/11

EphA2 Receptor Activation by Monomeric Ephrin-A1 on Supported Membranes

Qian Xu,[†‡§] Wan-Chen Lin,[†§] Rebecca S. Petit,[†§] and Jay T. Groves[†‡§*]
[†]Howard Hughes Medical Institute, Department of Chemistry and [‡]Biophysics Graduate Group, University of California, Berkeley, California; and [§]Physical Biosciences and Materials Sciences Divisions, Lawrence Berkeley National Laboratory, Berkeley, California

ABSTRACT The receptor tyrosine kinase EphA2 interacts with its glycosylphosphatidylinositol (GPI)-linked ephrin-A1 ligand in a juxtacrine configuration. The soluble ephrin-A1 protein, without its GPI membrane linker, fails to activate EphA2. However, preclustered ephrin-A1 protein is active in solution and has been frequently used to trigger the EphA2 receptor. Although this approach has yielded insights into EphA2 signaling, preclustered ligands bypass natural receptor clustering processes and thus mask any role of clustering as a signal regulatory mechanism. Here, we present EphA2-expressing cells with a fusion protein of monomeric ephrin-A1 (mEA1) and enhanced monomeric yellow fluorescent protein that is linked to a supported lipid bilayer via a nickel-decahistidine anchor. The mEA1 is homogeneously dispersed, laterally mobile, and monomeric as measured by fluorescence imaging, correlation spectroscopy, and photon counting histogram analysis, respectively. Ephrin-A1 presented in this manner activates EphA2 on the surface of MDA-MB-231 human breast cancer cells, as measured by EphA2 phosphorylation and degradation. Spatial mutation experiments in which nanopatterns on the underlying substrate restrict mEA1 movement in the supported lipid bilayer reveal spatio-mechanical regulation of this signaling pathway, consistent with recently reported observations using a synthetically cross-linked ephrin-A1 dimer.

INTRODUCTION

Eph receptor tyrosine kinases, through binding to either glycosylphosphatidylinositol (GPI)-linked or transmembrane ephrin ligands, are important regulators of cell adhesion, migration, and vascular development (1). Eph and ephrin interactions have been shown to both suppress and promote cancer formation by altering cell repulsion and migration (2). In particular, EphA2 and its GPI-linked ligand ephrin-A1 are important in maintaining many different tumor types (3). Overexpression of EphA2 in nontransformed mammary epithelial cells confers malignant transformation and tumorigenic potential (4,5). Decreasing expression of EphA2 can reverse metastatic behavior in immortal breast epithelial cell lines (6). In addition to these pro-oncogenic properties of overexpressed EphA2, this receptor has also been shown to suppress tumorigenesis. For example, EphA2 knockout mice are more susceptible to develop skin cancer upon exposure to known carcinogens (7). These findings, among others, have led EphA2 to become a target for cancer therapeutics.

EphA2 consists primarily of an intracellular kinase domain, an extracellular ligand-binding domain, and a transmembrane domain (8). Activation of EphA2 is marked by phosphorylation of the kinase domain (9) and can lead to receptor internalization and degradation through the recruitment of metalloproteases to the cell membrane (10). Ligand-induced receptor activation occurs upon the binding of EphA2 to its ephrin-A1 ligand presented on apposed cell membranes. Ligand binding is generally followed by dimerization of the receptor-ligand complex, oligomerization as a result of three distinct ligand binding sites on the receptor (11), and possibly larger scale cell surface reorganization (12). The clustering and subsequent endocytosis of EphA2 has been hypothesized as a method of regulating cell surface EphA2 levels (13). Ligand-induced receptor clustering has been proposed as a likely source of signal regulation that is independent of any conformational changes within the receptor and therefore a potential deregulatory mechanism in Eph-overexpressing tumors (14).

The hybrid live cell-supported lipid bilayer (SLB) junction, in which one cell surface in a juxtacrine signaling process is replaced by a SLB displaying ligands of interest, has proven to be an effective strategy to examine cell-cell signaling (12,15–18). SLBs can be formed by the spontaneous self-assembly of a phospholipid bilayer upon deposition of vesicles onto a silica support (19,20). The resulting membrane is continuous and fluid, with lipid lateral mobilities typically ranging from 1 to 3 $\mu m^2/s$ (21,22). GPI-linked proteins can be incorporated into SLBs without loss of mobility (23). In many cases, including the work presented here, protein linkage to the membrane by multivalent interactions between decahistidine tails on the protein and Ni-chelating lipids in the membrane is equally effective (24), and technically much simpler (25,26). We have recently used the live cell-SLB junction, functionalized with a preclustered EA1 ligand, to study properties of EphA2 signaling (12). This work revealed that the EphA2 signaling pathway is sensitive to the physical restriction of receptor-ligand movement over micron length scales within the plane of the cell-SLB interface. These results raise interesting hypotheses concerning the possibility of

Submitted April 27, 2011, and accepted for publication October 31, 2011.

*Correspondence: jtgroves@lbl.gov

Editor: Petra Schwille.

0006-3495/11/12/2731/9 $2.00

doi: 10.1016/j.bpj.2011.10.039

mechanosensing in relation to EphA2 signaling and they also underscore the importance of large-scale receptor assembly as a regulatory component of signaling. In this regard, however, the use of preclustered ligands is especially problematic because it essentially bypasses natural receptor assembly processes.

Eph receptors bind to ephrin ligands as a 1:1 complex (27) and can be activated by ephrin expressed on cell membranes or in a preclustered format (28). Soluble monomeric ephrin has generally been considered inactive. However, a recent report suggests that the media containing soluble and monomeric ephrin-A1, released from tumor cells, through possible cleavage processes, is capable of activating EphA2 in paracrine signaling (29). These contradictory findings underscore the complexity of Eph/ephrin interactions. Based on prior observations of inactive monomeric protein ligands becoming active in juxtacrine signaling from supported membranes, for example major histocompatibility complex in T cell receptor signaling (30) and neuroligin in neurexin signaling (31), we hypothesized that laterally mobile and monomeric ephrin-A1 presented on a supported membrane may activate the EphA2 receptor in the absence of synthetic cross-linking agents. Furthermore, this platform will provide a useful tool to study the signaling pathway and the effects of natural receptor clustering processes.

We constructed a fusion protein of monomeric ephrin-A1 (mEA1), enhanced yellow fluorescent protein (EYFP), and a 10-histidine (H10) tail. We have previously shown that H10 tails can form essentially irreversible multivalent linkage with Ni-chelating lipids in SLBs when assembled using kinetically controlled parameters (26). Fluorescence imaging of the mEA1-EYFP-H10 fusion protein in SLBs reveals that it is homogeneously distributed. Fluorescence correlation spectroscopy confirms that it is laterally mobile with a diffusion coefficient similar to that of the lipids, and photon counting histogram analysis reveals the protein to be predominantly monomeric on the membrane surface. The supported membrane-associated mEA1 activates the EphA2 receptor signaling pathway in live EphA2-expressing human breast cancer cells (MDA-MB-231), as measured by receptor phosphorylation and degradation. The soluble mEA1 is inactive in these experiments. Additionally, spatial mutation experiments in which nanopatterned structures on the underlying substrate are used to manipulate the movement and assembly of receptor-ligand complexes reveal spatio-mechanical influences over the EphA2 signaling pathway similar to recently reported observations using a synthetically cross-linked ephrin-A1 dimer, EA1-Fc (12). Large-scale EphA2/ephrin-A1 assembly occurs during activation even without any preclustering of the ligand and mechanical interference with this process leads to distinct alterations in cell behavior, as observed by cytoskeleton morphology and recruitment of the metalloprotease, ADAM10.

MATERIALS AND METHODS

This section has been moved to the Supporting Material.

RESULTS AND DISCUSSION

EA1 association with supported membranes is stable and properly oriented

The EA1 fusion protein is expressed by combining the human monomeric EA1 ectodomain sequence, along with the EYFP sequence (as a 1:1 construct between EA1 and EYFP), with an H10 tail on the C-terminus for linkage to Ni-chelating lipids, which are incorporated into the supported membrane at molar ratios ranging from 0.005 to 0.06 (Fig. 1 *A* and Fig. S1 in the Supporting Material). Multivalent Ni-histidine interactions are necessary to stably associate protein through this method (Fig. 1 *A inset*) (26). Typically, protein is incubated under carefully tuned kinetic control parameters to optimize for multivalent interactions. It is also generally necessary to allow a desorption period to remove weakly associated protein. Although equilibrium is never fully reached, stable multivalently bound His-tagged proteins can be achieved with reproducible results. A Ni-histidine dissociation curve is generated to show that the mutlivalent Ni-bound protein remains stably bound to the SLB for at least 16 h (Fig. 1 *B*). The protein linkage through histidine-chelated Ni interactions is confirmed by the addition of 100 mM EDTA, which strongly sequesters metal ions and leads to dissociation of protein bound in this manner (Fig. 1 *B*).

EA1 is mobile and predominantly monomeric in supported membranes

Fluorescence correlation spectroscopy (FCS) along with its counterpart photon counting histogram (PCH) analysis offer a powerful means to quantify the lateral mobility and the cluster size distribution of EA1 on the SLB surface (32). A typical time autocorrelation function of fluorescence intensity fluctuations from membrane-bound EA1 is plotted in Fig. 2 *A*. The data is fitted to an analytical expression of normal two-dimensional diffusion in a two-dimensional Gaussian illumination spot,

$$G(\tau) = \frac{1}{N_{ave}} \times \frac{1}{1+\tau/\tau_D}, \quad (1)$$

where N_{ave} represents the average number of independent molecules, τ is the time interval, and τ_D represents the characteristic residence time (33). Based on this model, the calculated diffusion coefficient for membrane EA1 is $2.3 \pm 0.2\ \mu m^2/s$. This value is typical for lipid diffusion in supported membranes (34) and also consistent with fluorescence recovery after photobleaching experiments (Fig. S2). Although tempting, one should not infer from this observation that the protein is monomeric. For FCS to

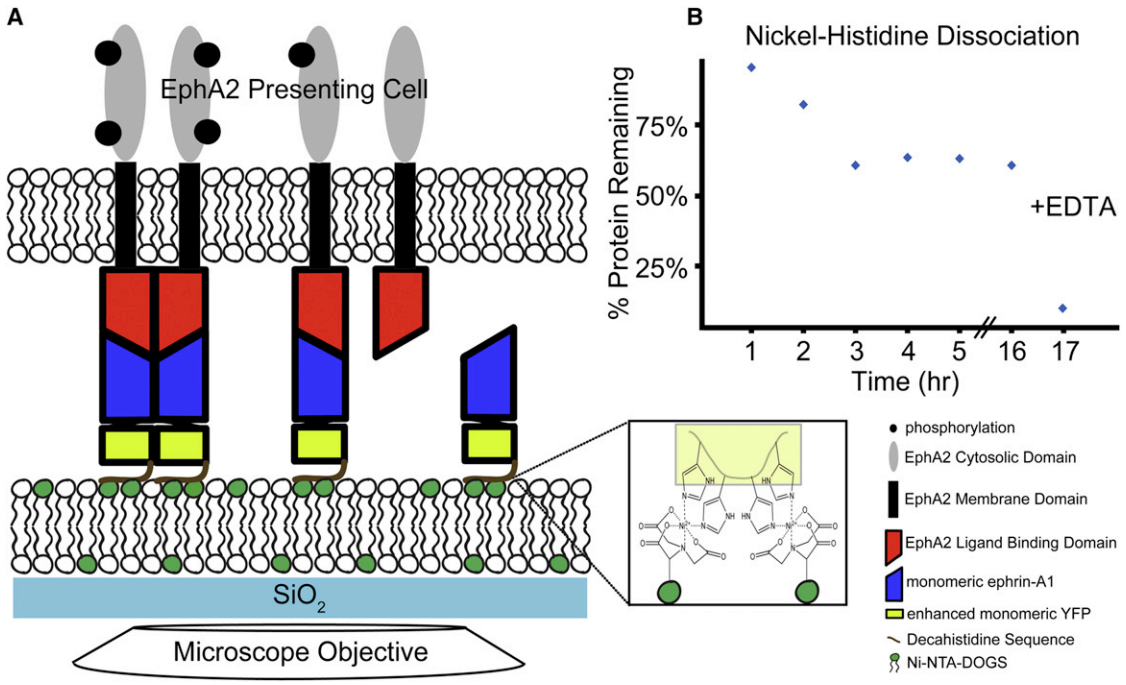

FIGURE 1 Schematic diagram of the experimental setup. (*A*) EphA2-expressing breast cancer cells are cultured on a SLB consisting of a tunable surface density of EA1 fusion proteins. This fusion protein is designed by linking the soluble portion of monomeric human ephrin-A1 with enhanced YFP that has an A206K mutation to prevent dimer formation. The inset shows the anchoring strategy, which is stable when the decahistidine sequence at the C-terminus of the fusion protein is chelating multiple Ni ions that are chelated by a tunable subset of lipids within the bilayer. (*B*) Ni-histidine dissociation curve shows that protein binding reaches a kinetically trapped state (*plateau in graph between 3 and 16 h*) that is stable and therefore insensitive to rinsing steps well beyond the timescale of experiments. The bilayer is incubated at 25°C for the entirety of the measurements except for an hour at 37°C in warm cell media after the first 2 h. The high temperature incubation period is performed to mimic the period after cells are introduced and then incubated at 37°C for an hour.

resolve two different species by their diffusion coefficients, a significant and well-defined difference in mobility is necessary (35). Because the EA1 is anchored to the membrane, its mobility is dominated by the membrane (36). As such, there is no well-defined scaling of molecular mobility with size and furthermore, the effective size of dimers, trimers, etc., is not at all clear (37). In light of these complexities, molecular mobility is an unreliable indicator of molecular size or state of clustering.

Direct analysis of the distribution of photon arrival times (PCH) emitted by the EYFP molecules (that are genetically fused to EA1) diffusing through the open confocal spot provides a significantly more sound method of determining the aggregation state of EA1 (Fig. 2 *B*). The fluorescence intensity fluctuations caused by the EYFP molecules yield a super-Poisson (Poi) distribution of photon counts arriving at the detector for a given time interval (38). By choosing a time interval that is short relative to the timescale for molecules to move through the laser spot, the PCH reflects the cluster size distribution and, importantly, is independent of mobility. The probability distribution of a single molecule, $p^{(1)}$, diffusing within a closed system, V_0, is expressed as

$$p^{(1)}(k;V_0,\varepsilon) = \int \mathrm{Poi}(k,\varepsilon\overline{PSF}(\vec{r}))p(\vec{r})d\vec{r}, \qquad (2)$$

where $\overline{PSF}$ is the scaled point spread function for synchronizing the PCH volume with the FCS volume, $p(\vec{r})$ represents the probability to find the molecule at position $\vec{r}$, k is the detected photon count, and ε is the molecular brightness of the molecule. For N independent and identical molecules, the joint probability distribution $p^{(N)}$ is calculated from consecutive convolutions of $p^{(1)}$. It is expressed as

$$p^{(N)}(k;V_0,\varepsilon) = \left(p_1^{(1)}\otimes\ldots\otimes p_N^{(1)}\right)(k;V_0,\varepsilon). \qquad (3)$$

It is numerically easier and equally accurate to select a reference volume (V_1) that is smaller than the reservoir (V_0) for deriving the PCH probability distribution so that the N value can remain small (38). The probability distribution for multiple molecules in an open system is the expectation value of $p^{(N)}$, which is weighted by the Poissonian probability, $p_{\#}(N)$, of observing N particles,

$$\prod(k;\overline{N}_{PSF},\varepsilon)\equiv\hat{p}(k;V_1,\overline{N},\varepsilon) = \left\langle p^{(N)}(k;V_1,\varepsilon)\right\rangle_N = \sum_{N=0}^{\infty} p^{(N)}(k;V_1,\varepsilon)p_{\#}(N), \qquad (4)$$

where the change from $\overline{N}$ to $\overline{N}_{PSF}$ reflects the selection of a V_1 that is smaller than V_0. This change does not affect the photon count probability because this probability of an

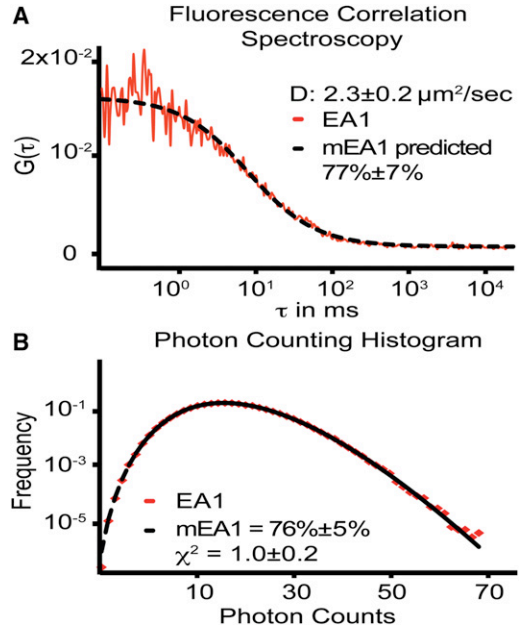

FIGURE 2 Characterization of mEA1-SLB surface heterogeneity and protein cluster size. (*A*) FCS is used to determine the heterogeneity of the surface. Values are fitted to a standard two-dimensional, single component curve. The diffusion constant calculated for the majority species is comparable to protein diffusion constants on cell membranes in vivo. A derivation of the autocorrelation function is used to relate the fraction of monomer to the average aggregation number (Q). From two independent FCS experiments, the derived function predicts that the fraction of monomeric species is 77 ± 7% for a Q value of three. (*B*) The PCH is best fit by a two species fit. The majority of the surface protein molecules (76 ± 5%) exhibit an average fluorescence intensity corresponding to a single EYFP flourophore, indicating that the majority of the species exists as monomer fusion proteins. This percentage is an average across three independent PCH experiments.

open system is independent of the volume V_1 as long as this probability can be referenced to the concentration of the molecule (38). In the case of membrane EA1, an accurate independent measurement of the surface density of EA1 is required to determine the N. This is achieved using quantitative fluorescence (QF) microscopy, which calibrates fluorescence from the membrane-bound analyte with fluorescent lipid standards with known membrane surface densities (39). Once this value is determined through QF, it is inserted into Eq. 4 and the resulting probability distribution is used to fit the membrane EA1 PCH. Because the PCH analysis has been experimentally demonstrated to be capable of resolving the aggregation state of fluorescent proteins (40), given an accurate value of N, both the average aggregation state (Q) and fraction (F) of monomeric EA1 can be determined from the best fit probability distribution, which has a local χ^2 value closest to one. Interestingly, the relationship between Q and F can be separately derived from the $G(0)$ of the autocorrelation function for a two-component model as

$$G(0) = \frac{Q + F(1-Q)}{N}, \tag{5}$$

where N is determined by QF measurements and $G(0)$ is calculated from Eq.1 as $1/N_{ave}$ (see the Supporting Material for derivation). Therefore, for a given integral value of Q, the F value can be predicted by Eq. 5.

The precision with which both FCS and PCH can determine the surface density is characterized using lipid bilayer standards (Fig. S3, *A–B*). FCS and PCH results are in precise agreement with each other as well as the known surface densities for boron-dipyrromethene (Bodipy) fluorescent dyes bound to the headgroups of phospholipid molecules incorporated into the bilayer at molar ratios of 0.0001, 0.0002, and 0.0004, (Fig. S3, *C–D*). For these standards, the fluorescent lipid molecules are expected to move as monomers, in which case N is simply the number of molecules. Using these three standard lipid membranes, QF is performed to determine the surface density of membrane EA1. Calibration of spectral properties between the YFP fluorophore on EA1 and the lipid standard is performed in solution to obtain a scaling factor (39) of 0.7 (Fig. S4 *A*). This relationship is linear at unsaturated fluorophore concentrations (39), enabling direct extrapolation to determine the EA1 surface density from measured fluorescence intensity (Fig. S4 *B*). When N determined from surface density measurements by QF is used to interpret the two species autocorrelation function (Eq. 5), 77 ± 7% of EA1 is found to be monomeric (mEA1) and the remaining 13% has a Q value of 3 (trimers). Similarly, the best probability distribution fit to the PCH data is a two species curve resulting in an average local χ^2 of 1.0 ± 0.2, corresponding to 76 ± 5% mEA1 with Q also equal to 3. The EA1 domain itself appears to be responsible for this clustering based on comparison to a similar fusion protein containing the extracellular domain of intercellular adhesion molecule 1 (ICAM) fused to YFP-H10 (ICAM-YFP-H10) (26,41). Both FCS and PCH analyses indicate ICAM-YFP-H10 to remain ~100% monomeric under similar conditions (Fig. S5 and Fig. S6).

To gauge the precision of this methodology to determine clustering state, probability distributions are also calculated for cases of several different aggregation states: solely monomeric, dimeric, or trimeric EA1. The respective residuals are plotted in Fig. S6. The resolution of PCH in distinguishing between aggregation states can be revealed in the poor χ^2 values of these cases. We conclude from two independent methods that the membrane-associated EA1 is predominantly monomeric.

EphA2 activation by membrane-associated EA1

After careful characterization of the membrane-associated EA1 surface, MDA-MB-231 cells, a highly invasive breast epithelial cancer cell line that overexpresses EphA2 (42),

are cultured on this surface under similar conditions used for the surface characterization, and its EphA2 activation is measured. EphA2 triggering by membrane-associated ephrin-A1 has been previously characterized through the phosphorylation and degradation of this receptor tyrosine kinase (12). These properties can be measured in two different manners: i), fluorescence microscopy to image immunostained signaling molecules colocalizing with EphA2, such as phosphotyrosine and the metalloprotease ADAM10, and ii), Western blot analysis to determine degradation and phosphorylation of EphA2. In this case, both methods are employed to determine EphA2 activation by membrane associated EA1.

First, to examine whether EphA2-expressing cells are responsive to changes in ligand concentration, MDA-MB-231 cells are incubated on different EA1 surfaces with different surface densities that are representative of typical cell surface concentrations of EA1. The EA1 surface density can be titrated by changing both the solution incubation concentration and the molar percent of Ni capturing lipids incorporated into the supported membrane (Fig. 3 *A*). The resulting mEA1 surface densities are measured using QF microscopy as previously described (39). After 10 min of incubation, the cells are fixed and permeabilized. Fluorescently labeled antibodies staining for EphA2 and phosphotyrosine are imaged using epifluorescence microscopy (Fig. 3 *B*). These representative images show the formation of EphA2 microclusters that colocalize with the microclusters of mEA1, imaged for the same cell. Similarly, phosphotyrosine immunofluorescence also colocalizes with mEA1 microclusters. The EphA2 receptor expressed on the membranes of MDA-MB-231 cells are interacting with membrane mEA1 proteins and there are high levels of phosphorylation, suggesting EphA2 activation. This colocalization is observed for mEA1 surface densities ranging from just a few molecules to hundreds of molecules/μm^2. The membrane mEA1 fusion protein presented to MDA-MB-231 cells is capable of initiating receptor phosphorylation over a wide range of surface densities.

Next, the lateral reorganization and clustering of the mEA1 fusion protein is examined over the course of an hour. This incubation time is previously shown to be a useful observation time for the central transport of membrane EA1 by EphA2 expressing cells (12). The EphA2 density on the surface of MDA-MB-231 is approximately several hundreds of molecules/μm^2; the surface density for mEA1 is fixed at a similar value for these experiments. Cells were fixed and permeabilized after incubations of 5, 10, 20, and 60 min for imaging (Fig. S7). At early time points (5 and 10 min), Eph-ephrin clusters are generally micron-sized or smaller and are randomly distributed across the cell-SLB interface. Within 1 h of cell engagement, these clusters coalesce into larger clusters that are transported to the center of the cell-SLB interface, resulting in a central contact zone several microns in diameter enriched in

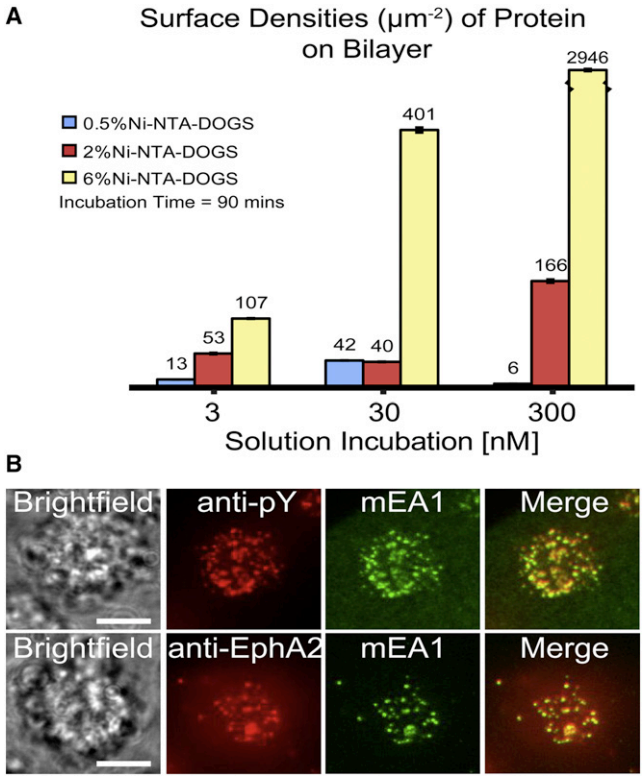

FIGURE 3 Surface density titration of mEA1 and immunofluorescence images of MDA-MB-231 cells. (*A*) The surface density of mEA1 is achieved by varying the solution incubation concentration above the bilayer and the molar ratio of Ni capturing lipids within the bilayer through kinetic control parameters. The surface density measurements are performed using quantitative fluorescence microscopy. (*B*) MDA-MB-231 cells are fixed and permeabilized after 15-min incubations on these surfaces. Antibodies against phosphorylated tyrosine residues (pY) and EphA2 are used to detect phosphorylation at the regions of mEA1 cluster formation and to stain for the presence of EphA2, respectively. For high mEA1 surface densities (thousands of molecules/μm^2), phosphorylated proteins are recruited to the mEA1 microclusters. At low mEA1 surface densities (hundreds of molecules/μm^2), EphA2 is also recruited. These results suggest that over a range of surface densities, phosphorylated proteins and EphA2 colocalize with mEA1 on the single cell level. A similar result is observed for EphA2 at high mEA1 surface densities and pY at low mEA1 surface densities; recruitment of both molecules occurs over a range of mEA1 surface densities (results not shown). Scale bars are 10 μm.

Eph-ephrin complexes. Temporal progression of ADAM10 recruitment to Eph-ephrin clusters is examined through staining cells with a fluorescently labeled anti-ADAM10 antibody. ADAM10 recruitment is a known step of the EphA2 degradation pathway, and is thought to enzymatically cleave the ephrin ligand from the ligand-presenting surface (10). At early time points (5 and 10 min), most of the ADAM10 is within the cell, well out of the focal plane of the objective, resulting in a blurred ADAM10 signal observed using epifluorescence microscopy. At later time points (20 and 60 min), we observe recruitment of ADAM10 to the EphA2-mEA1 clusters. A qualitative analysis of the fluorescence microscopy images suggest that

mEA1 leads to EphA2 phosphorylation and degradation as mediated by ADAM10. Furthermore, these results suggest that ADAM10 recruitment to Eph-ephrin clusters is a dynamic process. Despite the presence of a small minority of oligomeric EA1, the majority mEA1 is clearly active because essentially all of the available EA1 on the supported membrane is sequestered into EphA2 signaling clusters.

Finally, to contextualize these findings within the framework of classical biochemical techniques, Western blotting is used to examine EphA2 phosphorylation and degradation across a wide range of mEA1 surface densities and preclustered states (Fig. 4 and Figs. S8–S10). MDA-MB-231 cells are incubated on surfaces displaying different surface densities and aggregation states of mEA1, including both membrane bound as well as in solution. After 2 h incubations, the cells are lysed and the protein supernatant is analyzed. On the basis of the Western blot analysis, we interpret the lack of increased EphA2 downregulation as no EphA2 downregulation. Exogenous dimerization is introduced using an anti-green fluorescent protein mouse monoclonal IgG2a antibody to cross-link mEA1-eYFP-H10. A further degree of clustering is introduced through the addition of a goat anti-mouse IgG2a antibody. At low surface densities of EA1 (~100 molecules/μm^2) on the SLB, no significant EphA2 degradation or phosphorylation is observed regardless of the degree of EA1 cross-linking. Notably, this contrasts sharply with microscopy data, which indicates strong activation at similar densities. We speculate that Western analysis is not sufficiently sensitive to monitor signaling at these lower EA1 levels.

When the EA1 surface density is increased 10-fold (~1000 molecules/μm^2), EphA2 degradation and phosphorylation levels for mEA1 is measured at similar levels to those observed in response to soluble EA1-Fc, the synthetically cross-linked ephrin-A1 dimer. However, the membrane-bound antibody cross-linked mEA1, designed to mimic the EA1-Fc, is not as activating as the EA1-Fc presented on a supported membrane through a Ni-histidine linkage. To explain this discrepancy, the length scales of the two different cross-linking strategies need to be examined. For the antibody cross-linked mEA1, the distance between two antigen binding sites of an antibody is ~10 nm (43), and this spacing might be unfavorable for EphA2 activation. On the other hand, the EA1-Fc dimer is linked by a disulfide bond, which is ~0.1 nm in length. This observation is consistent with the small length scales required for the recruitment of proteins in Eph signaling that has been previously reported (44). Similar to previous reports of the inactivity of soluble monomeric ephrin-A1 (28), we also observed inactivity of the mEA1-eYFP-H10 in solution for both EphA2 degradation and phosphorylation Western blot analyses. Although fluorescence microscopy measurements suggest that EphA2 can be activated by membrane EA1 over a range of surface densities, Western blot analysis is only capable of detecting EphA2 activation at high densities of membrane EA1 because this analysis takes into account the fraction of total cell surface EphA2 that is downregulated. Our results suggest that activating a small fraction of EphA2 can initiate a full cellular response.

To extend observations beyond the MDA-MB-231 cell line, the central transport of membrane mEA1 by EphA2 expressing cells is also observed for other breast cancer cell lines (Fig. S11). After an hour incubation on supported membranes with EA1 surface densities of ~100 molecules/μm^2, a similar EA1-bound EphA2 transport leading to a central contact zone is observed. Immunofluorescence images of EphA2 show the receptor colocalizing with mEA1. The enchanced fluidity of the Ni-histidine anchoring strategy allows for a kinetically faster central transport as compared to the synthetically cross-linked ephrin-A1 dimer on supported membrane as demonstrated previously (12).

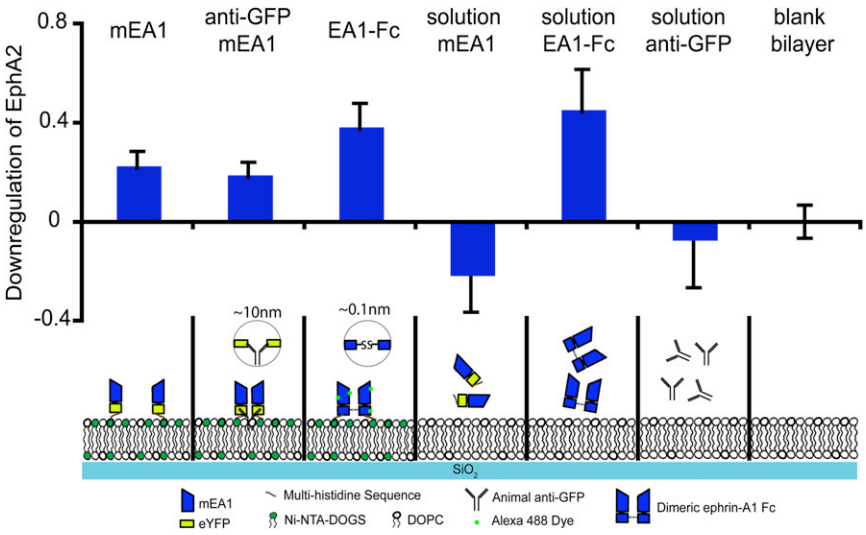

FIGURE 4 Western blots are analyzed from the lysate of MDA-MB-231 cells incubated on different surfaces and in different solutions. The blots are stained for the presence of EphA2. In this case, the degradation of EphA2 is represented by the intensity of an EphA2 band between 75 and 150 kDa. The lower the band intensity, the greater the receptor degradation. Intensity measurements of EphA2 bands are repeated for at least four unique Western blots and the results are averaged across the blots. Soluble mEA1, over a range of concentrations (results not shown), does not induce significant EphA2 degradation, whereas mEA1 on a SLB leads to EphA2 degradation. Antibody cross-linked mEA1 on a SLB leads to EphA2 degradation, although to a lesser degree than preclustered EA1-Fc. At low surface densities of mEA1, Western blot analysis is unable to detect significant EphA2 activation (Figs. S8–S10).

EphA2 signal regulation in MDA-MB-231 cells has spatio-mechanical dependency

Sensitivity of the EphA2 system to spatio-mechanical perturbation is tested using the spatial mutation strategy. Patterns of metal grids, prefabricated onto the underlying substrate, restrict the lateral mobility of membrane mEA1 as well as ligand-engaged EphA2 receptors on the live cell. Immunofluorescence images of phalloidin-labeled actin and ADAM10 detected with epifluorescence and total internal reflection fluorescence microscopies, respectively, show the altered downstream signals as a consequence of EphA2 spatial mutation. When Eph-ephrin clusters are laterally constrained within corrals larger than five microns in pitch, the actin cytoskeleton is concentrated in an annulus, immediately peripheral to the Eph-ephrin central assembly (Fig. 5 *A*), which is indicative of cell contraction from the ephrin-presenting surface. When grids with narrower pitches are prepatterned onto the underlying substrate, the cytoskeleton displays a spreading morphology, suggesting mesenchymal cell behavior (45). Using total internal reflection fluorescence, which excites fluorophores within 70–100 nm of the cell-SLB interface thereby eliminating a majority of the intracellular fluorescence signal (32), increasing ADAM10 recruitment is observed when Eph-ephrin transport is less hindered (Fig. 5, *B* and *C*). The density of EphA2 on the membrane surface is equal across the different pitched corrals, suggesting that EphA2 recruitment to the cell membrane is unaffected by the Cr grids (Fig. 5 *C*). These findings suggest that EphA2 signaling is sensitive to the lateral organization of membrane mEA1. Furthermore, this signaling pathway exhibits a dependency on the spatio-mechanical organization of the EphA2 receptor.

CONCLUSION

Monomeric ephrin-A1 displayed on a supported membrane successfully triggers EphA2 in living cells. Importantly, this system enables observations of natural receptor ligand clustering and assembly processes, as driven by the EphA2 receptor expressing cell. We affirm some fundamental observations concerning influences of mechanical constraints of ephrin-A1 ligand movement on EphA2 signaling, which had been originally reported using only chemically cross-linked ephrin-A1 ligands. The findings presented here confirm that the spatio-mechanical sensitivity we discovered in the EphA2 signaling pathway is not due to the chemical cross-linking of ephrin-A1 from using a streptavidin-biotin linkage. However, some differences in the kinetics of assembly are also noted between the two systems. Through

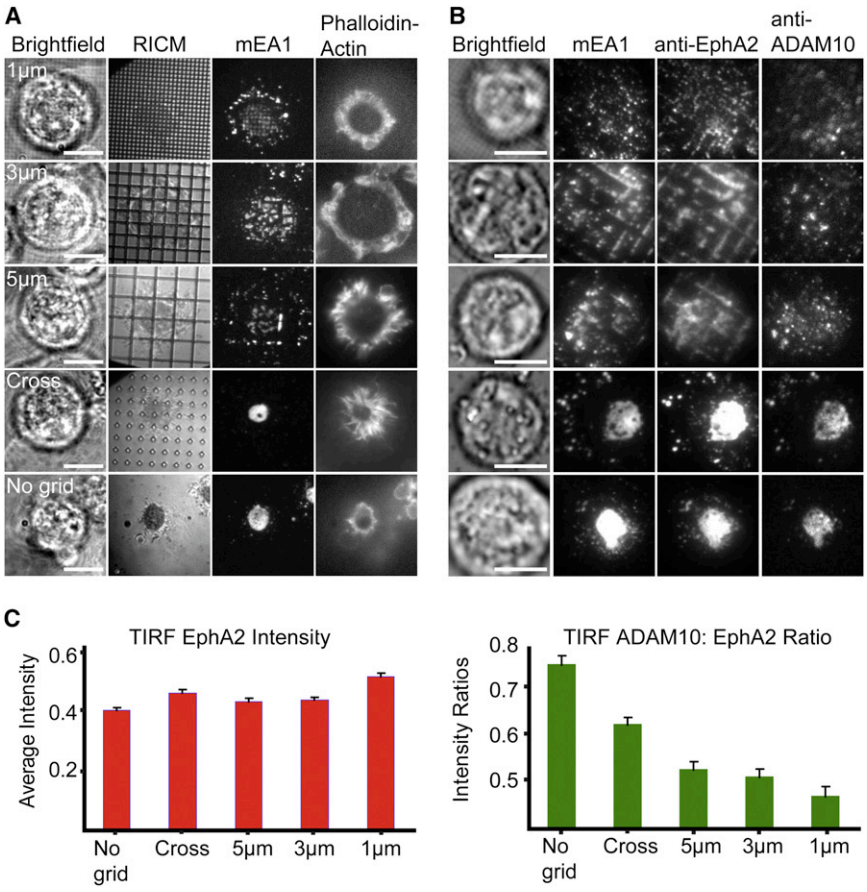

FIGURE 5 EphA2 pathway activated by mEA1 shows a spatio-mechanical regulatory component. (*A*) Ligand-induced EphA2 clustering is restricted with chromium barriers. Epifluorescence images show cytoskeleton annulus formation when transport is unrestricted and cytoskeleton spreading morphology when transport is restricted. (*B*) Total internal reflection fluorescence microscopy and (*C*) subsequent quantitative colocalization analysis of EphA2 to ADAM10 reveals that ADAM10 recruitment occurs only when receptor transport is unhindered. An average of 200 cells was analyzed for each grid pitch. The surface density of mEA1 used for these experiments is approximately hundreds of molecules/μm^2. Scale bars are 10 μm.

the use of a monomeric fluorescent fusion protein of ephrin-A1, we are able to examine the initial steps of Eph-ephrin clustering and transport that have been shown to play vital roles in signal transduction and is functionally altered in cancerous cells.

SUPPORTING MATERIAL

Eleven figures, Materials and Methods, and references are available at http://www.biophysj.org/biophysj/supplemental/S0006-3495(11)01261-6.

The authors thank Pradeep M. Nair and Michael P. Coyle for critical reading of the manuscript. The authors also thank Joe W. Gray for providing the Western blotting equipment and Odyssey Infrared Imaging machine.

This work was supported by the Director, Office of Science, Office of Basic Energy Sciences, Chemical Sciences, Geosciences, and Biosciences Division (Q.X.; hybrid synthetic-live cell interfaces) and the Materials Sciences and Engineering Division (R.S.P.; supported membrane substrates) of the U.S. Department of Energy (DOE) under contract no. DE-AC02-05CH11231. Patterned substrate fabrication was performed, in part, at the Molecular Foundry (or National Center for Electron Microscopy), Lawrence Berkeley National Laboratory (LBNL), and was supported by the Office of Science, Office of Basic Energy Sciences, Scientific User Facilities Division, of the U.S. DOE under contract no. DE-AC02-05CH11231. This work was also supported by the Laboratory Directed Research and Development Program of LBNL under U.S. DOE contract no. DE-AC02-05CH11231. Seed support for biomedical aspects of this work was provided by the U.S. Department of Defense DA Congressionally Directed Medical Research Program Idea Award BC102681 under U.S. Army Medical Research Acquisition Activity no. W81XWH-11-1-0256, with follow-on support provided by Award U54 CA143836 from the National Cancer Institute (NCI) beginning in 2009. The content is solely the responsibility of the authors and does not necessarily represent the official views of the NCI or the National Institutes of Health.

REFERENCES

1. Lackmann, M., and A. W. Boyd. 2008. Eph, a protein family coming of age: more confusion, insight, or complexity? *Sci. Signal.* 1:re2.
2. Mosch, B., B. Reissenweber, C. Neuber, and J. Pietzsch. 2010. Eph receptors and ephrin ligands: important players in angiogenesis and tumor angiogenesis. *J. Oncol.* 2010:135285.
3. Wykosky, J., and W. Debinski. 2008. The EphA2 receptor and ephrinA1 ligand in solid tumors: function and therapeutic targeting. *Mol. Cancer Res.* 6:1795–1806.
4. Kinch, M. S., and K. Carles-Kinch. 2003. Overexpression and functional alterations of the EphA2 tyrosine kinase in cancer. *Clin. Exp. Metastasis.* 20:59–68.
5. Zelinski, D. P., N. D. Zantek, …, M. S. Kinch. 2001. EphA2 overexpression causes tumorigenesis of mammary epithelial cells. *Cancer Res.* 61:2301–2306.
6. Carles-Kinch, K., K. E. Kilpatrick, …, M. S. Kinch. 2002. Antibody targeting of the EphA2 tyrosine kinase inhibits malignant cell behavior. *Cancer Res.* 62:2840–2847.
7. Guo, H., H. Miao, …, B. Wang. 2006. Disruption of EphA2 receptor tyrosine kinase leads to increased susceptibility to carcinogenesis in mouse skin. *Cancer Res.* 66:7050–7058.
8. Himanen, J. P., K. R. Rajashankar, …, D. B. Nikolov. 2001. Crystal structure of an Eph receptor-ephrin complex. *Nature.* 414:933–938.
9. Schlessinger, J. 2000. Cell signaling by receptor tyrosine kinases. *Cell.* 103:211–225.
10. Janes, P. W., N. Saha, …, D. B. Nikolov. 2005. Adam meets Eph: an ADAM substrate recognition module acts as a molecular switch for ephrin cleavage in trans. *Cell.* 123:291–304.
11. Smith, F. M., C. Vearing, …, A. W. Boyd. 2004. Dissecting the EphA3/Ephrin-A5 interactions using a novel functional mutagenesis screen. *J. Biol. Chem.* 279:9522–9531.
12. Salaita, K., P. M. Nair, …, J. T. Groves. 2010. Restriction of receptor movement alters cellular response: physical force sensing by EphA2. *Science.* 327:1380–1385.
13. Zhuang, G., S. Hunter, …, J. Chen. 2007. Regulation of EphA2 receptor endocytosis by SHIP2 lipid phosphatase via phosphatidylinositol 3-Kinase-dependent Rac1 activation. *J. Biol. Chem.* 282:2683–2694.
14. Himanen, J. P., L. Yermekbayeva, …, S. Dhe-Paganon. 2010. Architecture of Eph receptor clusters. *Proc. Natl. Acad. Sci. USA.* 107:10860–10865.
15. Grakoui, A., S. K. Bromley, …, M. L. Dustin. 1999. The immunological synapse: a molecular machine controlling T cell activation. *Science.* 285:221–227.
16. Mossman, K. D., G. Campi, …, M. L. Dustin. 2005. Altered TCR signaling from geometrically repatterned immunological synapses. *Science.* 310:1191–1193.
17. Manz, B. N., and J. T. Groves. 2010. Spatial organization and signal transduction at intercellular junctions. *Nat. Rev. Mol. Cell Biol.* 11:342–352.
18. DeMond, A. L., K. D. Mossman, …, J. T. Groves. 2008. T cell receptor microcluster transport through molecular mazes reveals mechanism of translocation. *Biophys. J.* 94:3286–3292.
19. Sackmann, E. 1996. Supported membranes: scientific and practical applications. *Science.* 271:43–48.
20. Richter, R. P., R. Bérat, and A. R. Brisson. 2006. Formation of solid-supported lipid bilayers: an integrated view. *Langmuir.* 22:3497–3505.
21. Machán, R., and M. Hof. 2010. Lipid diffusion in planar membranes investigated by fluorescence correlation spectroscopy. *Biochim. Biophys. Acta.* 1798:1377–1391.
22. Groves, J. T., N. Ulman, and S. G. Boxer. 1997. Micropatterning fluid lipid bilayers on solid supports. *Science.* 275:651–653.
23. Groves, J. T., C. Wülfing, and S. G. Boxer. 1996. Electrical manipulation of glycan-phosphatidyl inositol-tethered proteins in planar supported bilayers. *Biophys. J.* 71:2716–2723.
24. Groves, J. T., and M. L. Dustin. 2003. Supported planar bilayers in studies on immune cell adhesion and communication. *J. Immunol. Methods.* 278:19–32.
25. Dorn, I. T., K. R. Neumaier, and R. Tampé. 1998. Molecular recognition of histidine-tagged molecules by metal-chelating lipids monitored by fluorescence energy transfer and correlation spectroscopy. *J. Am. Chem. Soc.* 120:2753–2763.
26. Nye, J. A., and J. T. Groves. 2008. Kinetic control of histidine-tagged protein surface density on supported lipid bilayers. *Langmuir.* 24:4145–4149.
27. Lackmann, M., R. J. Mann, …, A. W. Boyd. 1997. Ligand for EPH-related kinase (LERK) 7 is the preferred high affinity ligand for the HEK receptor. *J. Biol. Chem.* 272:16521–16530.
28. Davis, S., N. W. Gale, …, G. D. Yancopoulos. 1994. Ligands for EPH-related receptor tyrosine kinases that require membrane attachment or clustering for activity. *Science.* 266:816–819.
29. Wykosky, J., E. Palma, …, W. Debinski. 2008. Soluble monomeric EphrinA1 is released from tumor cells and is a functional ligand for the EphA2 receptor. *Oncogene.* 27:7260–7273.
30. Boniface, J. J., J. D. Rabinowitz, …, M. M. Davis. 1998. Initiation of signal transduction through the T cell receptor requires the multivalent engagement of peptide/MHC ligands [corrected]. *Immunity.* 9:459–466.
31. Baksh, M. M., C. Dean, …, J. T. Groves. 2005. Neuronal activation by GPI-linked neuroligin-1 displayed in synthetic lipid bilayer membranes. *Langmuir.* 21:10693–10698.

32. Groves, J. T., R. Parthasarathy, and M. B. Forstner. 2008. Fluorescence imaging of membrane dynamics. *Annu. Rev. Biomed. Eng.* 10:311–338.

33. Lakowicz, J. R. 1991. Topics in Fluorescence Spectroscopy. Plenum Press, New York.

34. Moran, U., R. Phillips, and R. Milo. 2010. SnapShot: key numbers in biology. *Cell.* 141:1262–1262.e1.

35. Meseth, U., T. Wohland, …, H. Vogel. 1999. Resolution of fluorescence correlation measurements. *Biophys. J.* 76:1619–1631.

36. Saffman, P. G., and M. Delbrück. 1975. Brownian motion in biological membranes. *Proc. Natl. Acad. Sci. USA.* 72:3111–3113.

37. Naji, A., A. J. Levine, and P. A. Pincus. 2007. Corrections to the Saffman-Delbruck mobility for membrane bound proteins. *Biophys. J.* 93:L49–L51.

38. Chen, Y., J. D. Müller, …, E. Gratton. 1999. The photon counting histogram in fluorescence fluctuation spectroscopy. *Biophys. J.* 77:553–567.

39. Galush, W. J., J. A. Nye, and J. T. Groves. 2008. Quantitative fluorescence microscopy using supported lipid bilayer standards. *Biophys. J.* 95:2512–2519.

40. Müller, J. D., Y. Chen, and E. Gratton. 2000. Resolving heterogeneity on the single molecular level with the photon-counting histogram. *Biophys. J.* 78:474–486.

41. Hartman, N. C., J. A. Nye, and J. T. Groves. 2009. Cluster size regulates protein sorting in the immunological synapse. *Proc. Natl. Acad. Sci. USA.* 106:12729–12734.

42. Neve, R. M., K. Chin, …, J. W. Gray. 2006. A collection of breast cancer cell lines for the study of functionally distinct cancer subtypes. *Cancer Cell.* 10:515–527.

43. Murphy, R. M., H. Slayter, …, M. L. Yarmush. 1988. Size and structure of antigen-antibody complexes. Electron microscopy and light scattering studies. *Biophys. J.* 54:45–56.

44. Nievergall, E., P. W. Janes, …, M. Lackmann. 2010. PTP1B regulates Eph receptor function and trafficking. *J. Cell Biol.* 191:1189–1203.

45. Symons, M., and J. E. Segall. 2009. Rac and Rho driving tumor invasion: who's at the wheel? *Genome Biol.* 10:213.

EPHA2 – EPHRIN-A1 TRANSPORT IS FRUSTRATED BY NANOSCALE OBSTACLE ARRAYS, BUT ONLY IN INVASIVE CANCER CELL LINES

Theobald Lohmüller[1,3*], Qian Xu[2,3*], and Jay T. Groves[1,2,3]

Howard Hughes Medical Institute, Department of Chemistry[1], and Biophysics Graduate Group[2], University of California, Berkeley, California 94720, and the Physical Biosciences and Materials Sciences Divisions[3], Lawrence Berkeley National Laboratory, Berkeley, California 94720

*These authors contributed equally to this work.

E-mail: jtgroves@lbl.gov

Juxtacrine signaling interactions between the EphA2 receptor tyrosine kinase and its ephrin-A1 ligand contribute to healthy tissue maintenance and misregulation of this system is observed in 40% of human breast cancer. Hybrid live cell – supported membrane experiments, in which membrane-linked ephrin-A1 displayed in supported membranes interacts with EphA2 in living cells, have revealed large scale clustering of EphA2 – ephrin-A1 complexes as well as their lateral transport across the cell surface during triggering. Additionally, characteristics of these spatial reorganization processes vary between different breast epithelial cancer cell lines derived from different patients in ways that correlate with invasion potential. Here, we utilize 100nm spaced hexagonally ordered arrays of gold nanoparticles embedded within supported membranes to present defined obstacles to the movement and assembly of EphA2 clusters. Effectively, we perform size exclusion chromatography on EphA2 signaling clusters in live cell membranes. Analysis of ten different breast cancer cell lines reveals that EphA2 transport is most frustrated by nanoparticle arrays in the most highly invasive cell lines. These observations suggest that strong physical association among EphA2 receptors, as well as their assembly into larger clusters, correlates with and may contribute to the pathological misregulation of the EphA2 – ephrin-A1 pathway in breast cancer.

Metastasis, the spread of malignant tumor cells from a primary tumor to different locations, is the cause for over 90% of all cancer patient fatalities.[1] Correspondingly, therapeutic interventions that combat metastasis have significant potential to increase life expectancy. Metastasis is a multistage process that begins with invasion, which is the movement of cells from their primary tumor environment into adjacent tissue, and ends with the colonization of these cells at distant sites.[2] Physical properties of the microenvironment surrounding the tumor cells such as interstitial pressure and tensional force, in cooperation with the intrinsic biochemistry of the cells, contribute to diseased behavior.[3, 4] Errant intracellular signaling processes, especially those associated with receptor tyrosine kinases (RTK), have also been identified as significant factors in cancer.[5-7]

The Eph receptors are a family of RTKs that bind to ephrin ligands in a juxtacrine configuration, which are involved in the positioning, adhesion, and migration of cells during early development.[8, 9] In later development, they maintain their role in cell-positioning and regulating cell-cell repulsion and adhesion interactions.[8] As part of a chematactic guidance system, in neural stem cells, Eph receptors are involved in recognizing and transmitting signals from the extracellular microenviroment which allows the cells to perform signature stem cell activities such as self-renewal and differentiation[10], and are therefore sensitive to the biophysical layout and biochemical landscape of the microenvironment.[11] Eph receptors and their ephrin ligands are also points of corruption in cancer cell invasion, metastasis, and angiogenesis.[12] EphA2, for example, which binds its monomeric ligand ephrin-A1 on an apposed cell membrane, is overexpressed in over 40% of all breast cancers[13] and EphA2 overexpression is highly correlated to tumor metastasis.[14] At expression levels similar to those found in cancer cells, Eph clustering can lead to transforming phenotypes and is thought to be responsible for metastatic behavior in patient tissue samples.[15, 16] As a result, much attention has been directed towards developing therapeutics targeting EphA2. Strategies include promoting the elimination of EphA2 by antibody stimulation[17] or targeting cancer cells to destruction by the native immune system with a bispecific antibody that recognizes EphA2 and the T cell receptor/CD3 complex on T cells.[18] Despite its known role in cancer and its potential as a target, what precisely goes wrong with the EphA2 signaling pathway to contribute to cancer remains unclear. In general, the receptor itself is not mutated.[13]

We have previously reported that ligand-induced spatial reorganization of the EphA2 receptor correlates with invasion potential.[19] These studies further revealed that downstream processes in the EphA2 signaling pathway, namely cytoskeleton reorganization and recruitment of the ADAM10 protease, are modulated by physical constraints imposed on receptor movement.[19, 20] EphA2 signaling is sensitive to physical characteristics of the environment, such as tissue stiffness, and this EphA2-mediated mechanosensing may be more significantly deregulated in the most invasive cancer cell lines. If these insights prove to be true, then therapeutic strategies that directly target mechanical aspects of EphA2 signaling may be effective.

In order to better understand the spatio-mechanical aspects of EphA2 signaling, we employ ordered arrays of gold nanoparticles embedded within supported membranes to present defined obstacles to the movement and assembly of EphA2 clusters.[21] Effectively, size-exclusion chromatography is performed on the EphA2 signaling clusters in living cell membranes. Ten different cell lines, with increasing invasion potentials, are studied to determine the freedom with which EphA2 clusters move through the ~100nm spaced array of fixed gold nanoparticle obstacles. In these experiments, a supported membrane is formed on a glass substrate with a preformed nanoparticle array, resulting in a continuous and fluid supported lipid bilayer membrane that surrounds the fixed array of nanoparticles. Ephrin-A1 ligands can be bound to the mobile membrane (via Ni-poly histidine interactions)[20, 22], to the nanoparticles (thereby becoming immobile)[21], or to both.

In the absence of physical constraints, triggering of EphA2 by mobile ephrin-A1 in fluid supported membranes results in large-scale clustering of EphA2-ephrin-A1 complexes, followed by their inward radial transport within the plane of the interface, and ultimate endocytosis.[19, 20] The lateral transport of EphA2-ephrin-A1 is readily imaged by fluorescence microscopy. This spatial transport, and the degree to which it is frustrated by the nanoparticle arrays, is our observable. Analysis of ten different breast cancer cell lines reveals that the most highly invasive cells also exhibit the most frustrated EphA2 transport through the gold nanoparticle obstacles. Stronger physical association among EphA2 receptors, as well as their assembly into larger clusters, correlates with and may contribute to the pathological misregulation of the EphA2 – ephrin-A1 pathway in breast cancer.

To prepare the nanoparticle/supported membrane substrate, arrays of gold nanoparticles are generated on top of a glass coverslip through block copolymer nanolithography.[21, 23] Only half of one side of the glass surface is decorated with the gold nanoparticles by dip-coating the coverslip half way into the polymer solution. The parameters of the nanopattern are fixed at an interparticle distance of ~100nm and a particle size of ~7nm, matching the thickness[24] of the supported membrane (Fig. 1A).[25] A supported lipid bilayer (SLB) is formed on the bare parts of the glass surface in between the nanoparticles through vesicle fusion.[26] Proteins are selectively tethered to either the nanoparticles or to the phospholipid membrane via Ni-NTA/His-tag binding (Fig. 1B).[21] The ephrin-A1 (EA1) fusion protein is designed by genetically fusing the ectodomain of human monomeric ephrin-A1 with a monomeric fluorescent Eos[27] and a sequence of ten histidines on the C-terminus. EphA2 expressing cancer cells can be activated by homogeneously distributed monomeric histidine-tagged ephrin-A1 ligands anchored to a supported bilayer.[20] The presence of the nanoparticle array is found to have no effect on neither the formation nor the fluidity of the bilayer (Fig. 1C).[21]

Since only half of the substrate is covered with nanoparticles while the bilayer is covering the whole glass surface area, the platform offers the unique flexibility to generate three different scenarios of EA1 presentation for live cell studies (Fig. 2): *i*) mobile EA1, with EA1 only anchored to the SLB (nanoparticles are not functionalized), *ii*) immobile EA1, with EA1 only tethered to the nanoparticles (SLB is not functionalized), and *iii*) hybrid EA1, with mobile and immobile EA1 tethered to the SLB and nanoparticles, respectively. Since the molar ratio of the Ni-NTA lipids in the bilayer can be tuned to achieve a high surface density of mobile membrane-associated EA1 ligands, the combination of supported membrane and nanoparticles in one configuration yields a surface on which the majority of EA1 ligands are mobile, while a much smaller fraction of the same protein is immobilized through linkage to the nanoparticles. To control for nonspecific cell – surface interactions, a substrate without EA1 is prepared.

MDA-MB-231 cells, a highly invasive breast epithelial cancer cell line, were deposited on surfaces with different presentations of EA1. After one hour the cells were imaged with reflection interference contrast microscopy (RICM) to observe the regions of tightest adhesion between the cell membrane and the supported bilayer interface (Fig. 2). In case of completely mobile EA1 presentation (no EA1 bound to nanoparticles), a tight central contact region between the cell membrane and the SLB on the glass and the nanoparticle side was observed by RICM

(Fig. 2A). This central contact region also represents regions of highest EA1 fluorescence intensity, indicating an EphA2 driven transport process associated with activation in the MDA-MB-231 cells which has been discussed in previous reports.[20] The presence of gold nanoparticles embedded in the membrane does not lead to any measureable effect on cell behavior. In order to investigate if a completely immobile ligand presentation will lead to a different outcome, the MDA-MB-231 cells were deposited on a substrate presenting only immobile EA1. Here, cell spreading and the formation of filopodia protrusions were observed (Fig. 2B).[28] The cells line up perfectly along the edge of the nanoparticle pattern. Scanning electron micrograph images show individual cells reaching out to individual EA1 coated nanoparticles (Fig. 2E-F). No cells were found to attach nonspecifically to the unlabelled bilayer (Fig. 2B, D). To verify that cell attachment to the nanoparticles is specific, cells were placed on a surface with Ni-NTA functionalized nanoparticles but without EA1. Most of the cells were easily rinsed away. These results confirm that the MDA-MB-231 cells interact with the substrate in an EA1-dependent manner.

The experiment was repeated with a substrate displaying both, mobile and immobile EA1 simultaneously in order to determine which adhesion phenotype would prevail (centralized contact junction or spreading). Two distinctly different morphologies were observed on the same glass surface. The cells on the nanoparticles are found to display a spreading morphology similar to cells cultured on a substrate with only immobile EA1 (Fig. 2C). In contrast, the same batch of cells, on the side without any nanoparticles, show a centralized contact region as expected on a completely mobile EA1 surface. We conclude from these results that the spreading phenotype, observed on the hybrid side, is caused by the presence of nanoparticle-bound immobile EA1 ligands.

To determine if EphA2 signaling molecules are recruited to the cell membrane – supported membrane interface, immunostained antibodies against EphA2, a disintegrin and metalloprotease 10 (ADAM10), and talin were imaged with total internal reflection microscopy (TIRFM). The actin cytoskeleton was stained with fluorescently-labeled phalloidin. ADAM10 and talin are proteins that are involved in EphA2 signaling and cytoskeleton reorganization, respectively. The former is a metalloprotease that is known to mediate the detachment of ephrin from the ephrin-expressing cell membrane upon binding to Eph.[29] Talin is a cytoskeletal protein that is commonly found in regions within cell-cell junctions.[30] Immunostained cells on a

substrate with mobile EA1 presentation showed EphA2, ADAM10, and talin all colocalizing with the EA1 in the center of the SLB-cell interface (Fig. 3 – Glass Side). Actin forms an annulus around the EA1 in the center, consistent with previous reports of central transport of EA1-bound EphA2 in the MDA-MB-231 cells.[19, 20] On the nanoparticle side, in the hybrid mobile/immobile scenario, fixed MDA-MB-231 cells reveal the formation of actin protrusions studded with EphA2 clusters (Fig. 3 – Nanoparticle side). ADAM10 and talin molecules are randomly distributed throughout the cell – supported membrane interface.

These results confirm that the distinct differences in cellular morphology and molecular recruitment between the same batch of MDA-MB-231 cells cultured on the hybrid EA1 or mobile EA1 side of the same substrate are due to the presence of immobile EA1 molecules. Despite of the presence of laterally mobile EA1, the MDA-MB-231 cells do not transport EA1/EphA2 clusters to the center. Instead, all centralized radial transport breaks down and the clusters are distributed along the cell membrane – supported membrane contact area wherein individual cellular protrusions interact with immobile EA1 preferentially (Fig. 3 – Nanoparticle Side).

To test whether the sensitivity of MDA-MB-231 cells in detecting small portions of immobile EA1 in the hybrid configuration is related to the high invasive properties of this particular cell line, the experiments were repeated with a non-invasive epithelial cancer cell line, MCF10A, which has comparable EphA2 mRNA expression as the MDA-MB-231 cells but is reportedly non-invasive and non-tumorigenic.[28] After depositing both cell lines, individually, on immobile ephrin-A1 surfaces with the same incubation, fixation, and staining conditions, MCF10A cells show a distinctively different phenotypefrom that of MDA-MB-231 cells (Fig. 4). On a substrate displaying only mobile ephrin-A1 on both the glass side and the nanoparticle side, MCF10A cells remain attached after rinsing steps, transporting EA1 into a central adhesion domain where EphA2 is also concentrated (Fig. 4A – mobile). These cells do not attach to nor interact with the substrate displaying only immobile EA1. After rinsing steps, the MCF10A cells are mostly detached from the immobile EA1 surface. When the two cell lines were individually placed on substrates displaying hybrid EA1 configurations, we observed no change in EphA2 transport by the MCF10A cells in response to EA1 immobilized nanoparticle obstacles (Fig. 4A – hybrid), in stark contrast to the response of the MDA-MB-231 cells (Fig. 4B – hybrid). While the MDA-MB-231 cells showed a clear and consistent difference between the glass side and the

nanoparticle side in terms of EphA2 clustering phenotype, no difference was observed for the MCF10A cells. MCF10A cells can centrally transport ligand-bound EphA2, seemingly unhindered by the presence of immobile ephrin-A1, while the MDA-MB-231 cells display distributed clusters of EphA2, whose larger sizes are excluded by the nanoparticles arrays, throughout the cell contact area (Fig. 4A,B – hybrid).

At this point we would like to emphasize that in the hybrid configuration, only a small percentage of the total EA1 amount is immobilized. This is important to consider since a majority of EA1 available to the cells is still mobile. Furthermore, the amount of mobile EA1 available to each cell is virtually unlimited due to its physical tether to the lipid bilayer, which renders it highly mobile and therefore easily transportable, while the surface density of immobile EA1 is practically limited by the number of nanoparticles underneath the cell. The large ratio of mobile EA1 to immobile EA1 in the hybrid configuration necessitates different physical conditions of EphA2 on the respective cell surfaces in order to sense the presence of the minor fraction of immobile EA1. One reason might be the presence of large EphA2 clusters on the cell surface of the highly invasive MDA-MB-231 cells. Ligand-independent EphA2 cluster formation on the surfaces of invasive cancer cells has been previously hypothesized as a possible cause for invasiveness.[15] In the presence of immobile EA1 functionalized on nanoparticles, individual EphA2 molecules in these pre-formed clusters can bind to individual EA1 on the nanoparticles, thus restraining the central transport of EA1-bound EphA2. The spreading behavior on the hybrid side of the substrate and the sensitivity to immobile EA1 could thus be an observation for highly invasive breast cancer cells.

To determine if the affinity of EphA2 cluster binding to small fractions of immobile EA1 follows a measurable trend, we extended our observations to eight more cancer cell lines, with varying degrees of invasion potentials, EphA2 protein expression and mRNA levels, tumorigenicities, and metastatic capabilities. The results for all ten cell lines are summarized in Figure 5. Each cell line was individually placed on substrates presenting hybrid EA1. The EphA2 clustering per cell line was measured by normalizing the EphA2 radial profiles of cells on the hybrid side to the EphA2 radial profiles of cells of the same cell line on the mobile side. This normalization eliminates errors introduced by cellular or experimental variability such as different EphA2 expression levels or variations in the staining protocol across all of the experiments. This procedure also highlights a powerful advantage of our approach that data

acquisition for both, experiment and control, are measured from the same glass surface under identical conditions and with the same batch of cells. Furthermore, the normalized EphA2 radial transport is correlated to the invasion potentials of the individual cell lines[28] (Fig. 5A).

EphA2 receptor is centrally transported for all ten cell lines on the control side displaying only mobile EA1. On the hybrid surface, the EphA2 central transport remains unhindered in the presence of immobile EA1 for five of the cell lines with low invasion potentials. However, with increasing invasion potential values, the EphA2 transport becomes interrupted and instead, small EphA2 clusters are distributed across the interface between the cell and the hybrid surface (Fig. 5B).

The correlation of the EphA2 clustering phenotype with the corresponding invasion potential of the cancer cell lines supports and underscores past hypotheses about the role of increased concentration EphA2 cluster formation in invasive cancers.[15, 16, 31, 32] Our results support a model that EphA2 clusters are preformed on the surface of invasive tumor cells to increase transport efficiency and quickly trigger cellular response. As a consequence, these highly invasive cells are particularly sensitive to immobilized EA1. EphA2 molecules might also be binding to EA1 as small oligomers but are aggregating more quickly in the invasive cells and therefore, they are hindered by the immobile EA1 obstacles. In this case, however, EA1 microclusters would form in addition to the EphA2 microclusters and therefore, when imaged together, they would colocalize. This is not observed. Instead, EphA2 microclusters are visible while the EA1 molecules either coalesce in the center by binding to EphA2 or are invisible. In light of this, we propose a model mechanism for the binding and unbinding of large EphA2 clusters to individual EA1 molecules functionalized on nanoparticles (Fig. 6).

When breast cancer cells are deposited on a mobile, membrane-associated EA1 surface, EphA2 receptors bind to available EA1 molecules and through a cytoskeletal driven mechanism, concentrate the EA1-bound EphA2 in the center of the SLB-cell junction. In the case of preformed EphA2 clusters consisting of tens of EphA2 receptors, through binding to individual EA1 molecules on nanoparticles, the central transport of the entire cluster is hindered. In these large clusters, when one EphA2 unbinds from the EA1 on a nanoparticle, another receptor can immediately take its place (Fig. 6A-C). In non-invasive cells, EphA2 receptors are not preclustered, and therefore the binding of individual EphA2 receptors to single immobile EA1

ligands results in comparably weaker cell membrane-nanoparticle interactions (Fig. 6D-E). EphA2 receptors will interact with mobile EA1 surrounding the immobile EA1.

EphA2 cluster formations on the surface of breast cancer cells are revealed when they are presented with a hybrid configuration of ephrin-A1 achieved by combining nanotechnology with supported membrane technology. This hybrid platform is uniquely suited to reveal a pre-existing condition that is only observed for cancer cell lines with the highest invasion potentials and therefore can be exploited to distinguish single cells from each other based on EphA2 clustering phenotypes. By simultaneously presenting mobile and immobile ephrin-A1 ligands on one substrate, we are able to perform size exclusion analysis in live cell membranes, and observe the presence of large, preformed EphA2 clusters on the surface of breast cancer cell lines. EphA2 clusters sensitizes the cells to detect and interact with immobilized EA1 ligands presented on nanoparticles, promoting cell spreading and adhesion. Remarkably, only highly invasive cancer cells show a strong binding affinity to immobilized ligands on the hybrid configuration. These findings suggest that tumor malignancy is not simply the result of EphA2 overexpression but perhaps a consequence of ligand independent receptor-receptor oligomerization on the cell surface. Large clusters of membrane receptors which allow cells to apply a mechanical force to its environment has been shown to facilitate tissue invasion and cell migration to initiate metastasis.[33] Potentially, this platform can be utilized to predict cancer invasion and metastasis, on a single-cell level, within a tumor population.

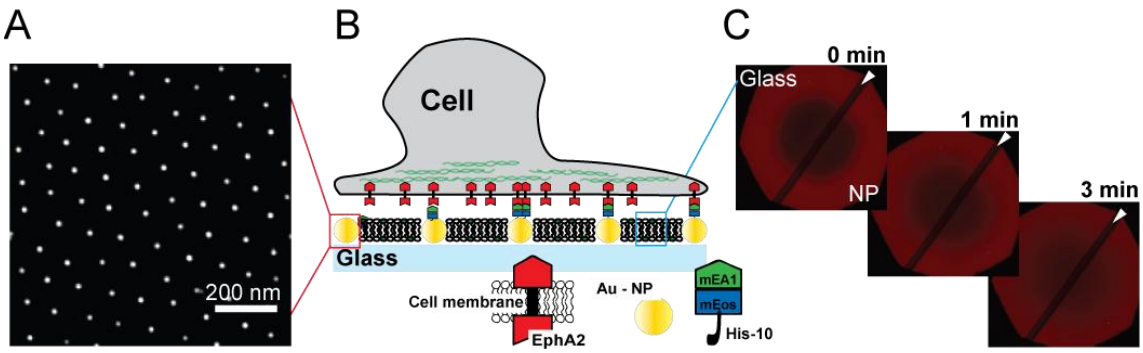

Fig. 1 Schematic of the experimental approach. **A)** Scanning electron micrograph of gold nanoparticles (Au-NP) on the surface of a glass coverslip. **B)** Schematic of the nanoparticle–supported lipid bilayer (SLB) platform: cancer cells expressing EphA2 deposited on this surface can interact with molecules of EA1 tethered to the nanoparticles or to the lipids with the SLB. **C)** Fluorescence recovery after photobleaching (FRAP) images at different time points show the recovery of a Texas Red DHPE SLB across the entire glass coverslip. This reveals that the membrane fluidity is not affected by the presence of the nanoparticles. The dark diagonal stripe (indicated by the white arrow) across the FRAP images is a result of the dipping process for nanoparticle functionalization and depicts the border between the bare glass side and the nanoparticle patterned side.

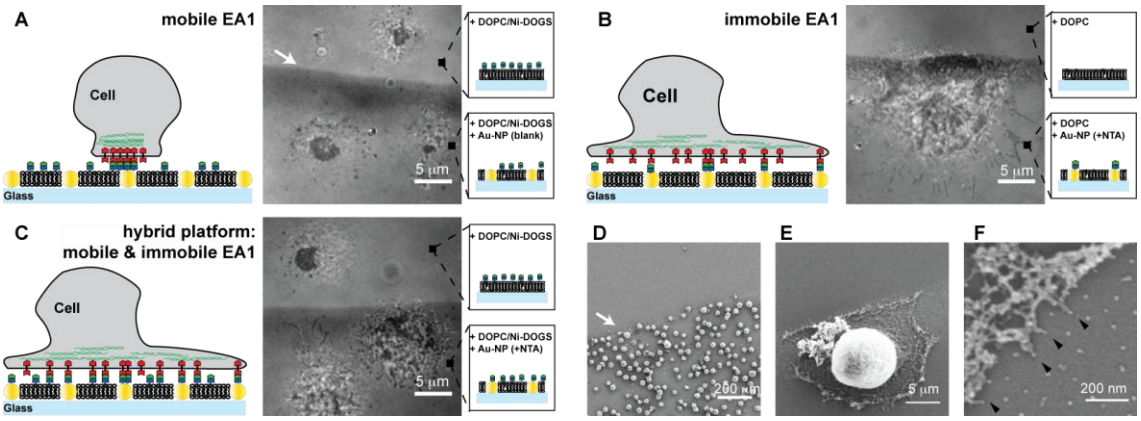

Fig. 2 MDA-MB-231 cells are placed on substrates with different ephrin-A1 (EA1) presentations. The combination of supported membrane formed on a glass coverslip with patterned nanoparticles (NP) on half of the surface yields three unique scenarios of EA1 presentation. **A)** In the case of ***mobile EA1***, only the phospholipids are functionalized with ligand molecules through a bilayer comprising 98% DOPC and 2% Ni-DOGS. Reflection interference contrast microscopy (RICM) image of MDA-MB-231 cells placed on a mobile EA1 surface is shown. Cells form a tight contact area with the supported membrane displaying mobile EA1 on both the nanoparticle patterned side as well as the glass side. These results indicate that the presence of blank NP does not cause any unspecific cell-substrate interaction. **B)** EA1 is selectively bound to the NP in case of an ***immobile EA1*** scenario. The bilayer is formed from 100% DOPC and does not contain any capturing lipids for the EA1. RICM image of cells placed on immobile EA1 surface shows a spreading morphology and filopodia protrusions. Remarkably no cells were attached to a pure bilayer. **C)** ***Hybrid platform*** refers to the case in which both the phospholipids and nanoparticles are individually patterned with ephrin-A1. Cells deposited on the hybrid platform show two distinct behaviors. MDA-MB-231 cells on the bare glass side that displays mobile EA1 forms the same central contact region as cells placed on a *mobile EA1* surface. The cells on the *hybrid platform* spread out, forming protrusions, similar to cells on the *immobile EA1* surface. **D-F)** Scanning electron micrograph (SEM) of MDA-MB-231 cells on the *immobile EA1* substrate. Cells are preferentially interacting with the nanoparticle side since the phospholipids are not functionalized with EA1. Higher magnification SEM images reveal that individual cell protrusions are interacting with single nanoparticles (black arrows).

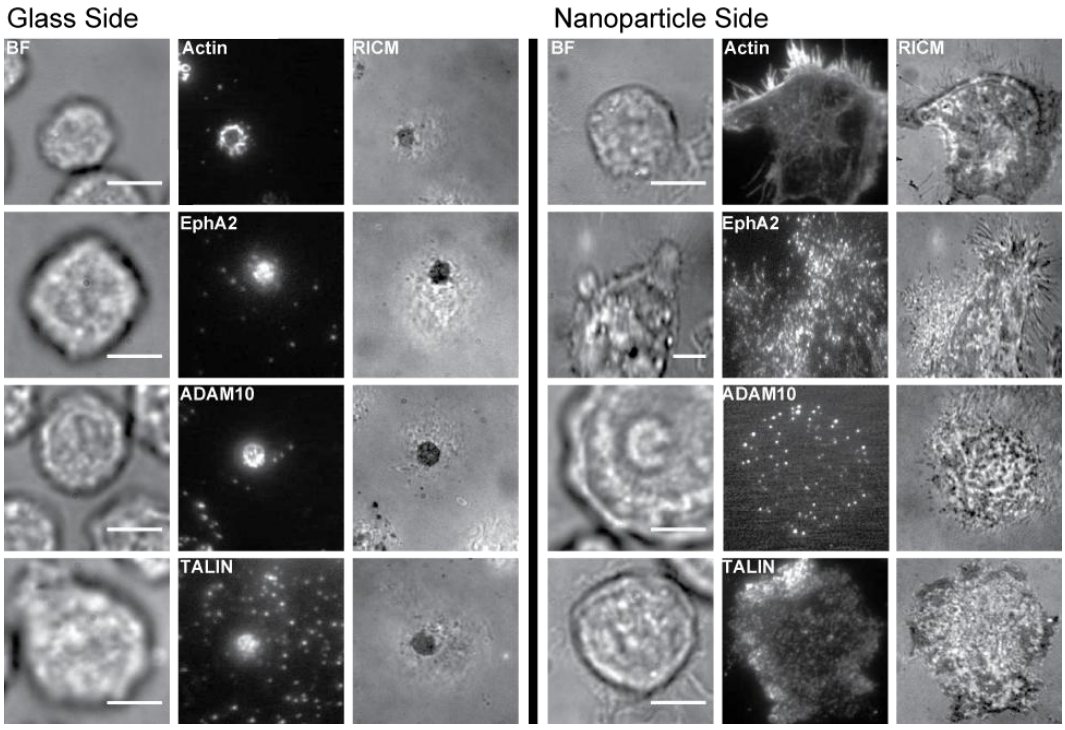

Fig. 3 MDA-MB-231 cells deposited on the hybrid platform are stained with phalloidin to image F-actin, and immunofluorescence is used to image EphA2, ADAM10, and talin. The images are taken using total internal reflection fluorescence microscopy. Glass side represents the side of the substrate displaying only laterally mobile, membrane-bound ephrin-A1. EphA2, ADAM10, and talin are all co-localized with the central adhesion domain imaged with RICM. This also represents the regions of highest EA1 concentration. Actin forms an annulus around the center. Nanoparticle side refers to the *hybrid platform*. Here, the immunostained molecules are spread across the cell-SLB interface in all cases. Scale bars are 10 microns.

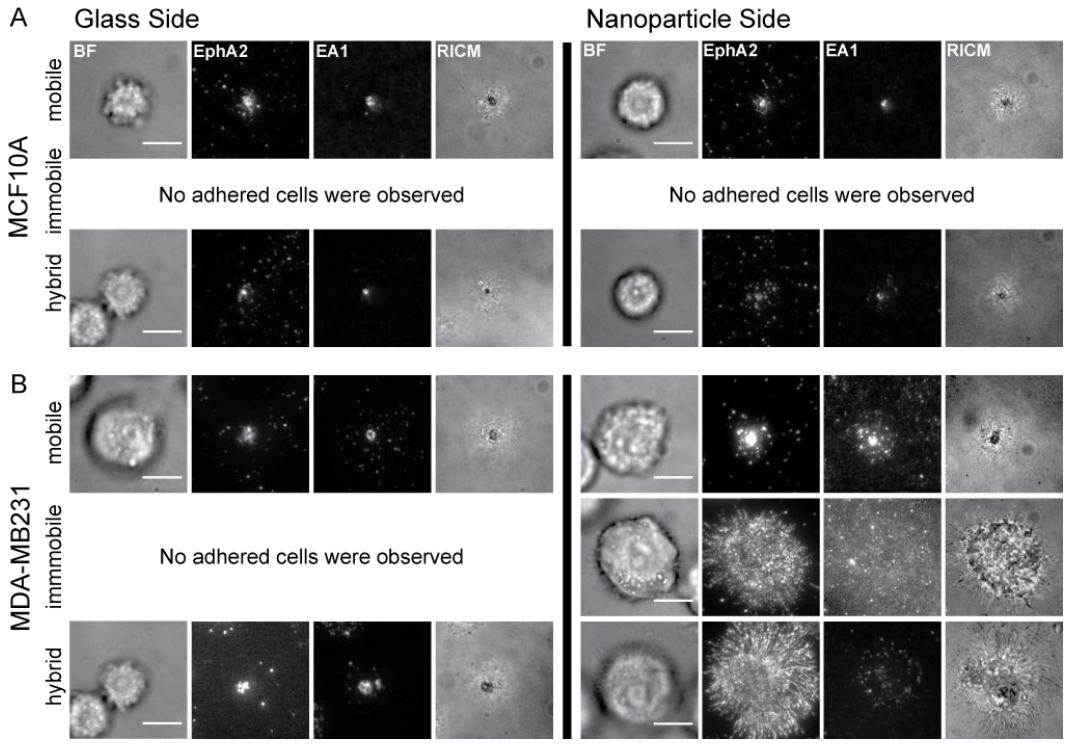

Fig. 4 Comparison between MCF10A and MDA-MB-231 cells placed on substrates with three different EA1 configurations. **A)** When MCF10A cells are placed on the *mobile EA1* surface, ligand-bound EphA2 is centrally transported. MCF10A cells detach from the substrate with *immobile EA1* after rinsing steps during fixation and permeabilization processes. When MCF10A cells are incubated on the *hybrid platform*, ligand-bound EphA2 complexes are centrally transported on both the glass side and the nanoparticle side. **B)** MDA-MB-231 cells incubated on a *mobile EA1* surface display a similar central transport and concentration of ligand-bound EphA2 on both the glass and the nanoparticle side. When placed on an *immobile EA1* substrate, the cells attach and spread out, selectively interacting with the nanoparticles. MDA-MB-231 cells cultured on the *hybrid platform* show two distinct phenotypes. Scale bars are all 10 microns.

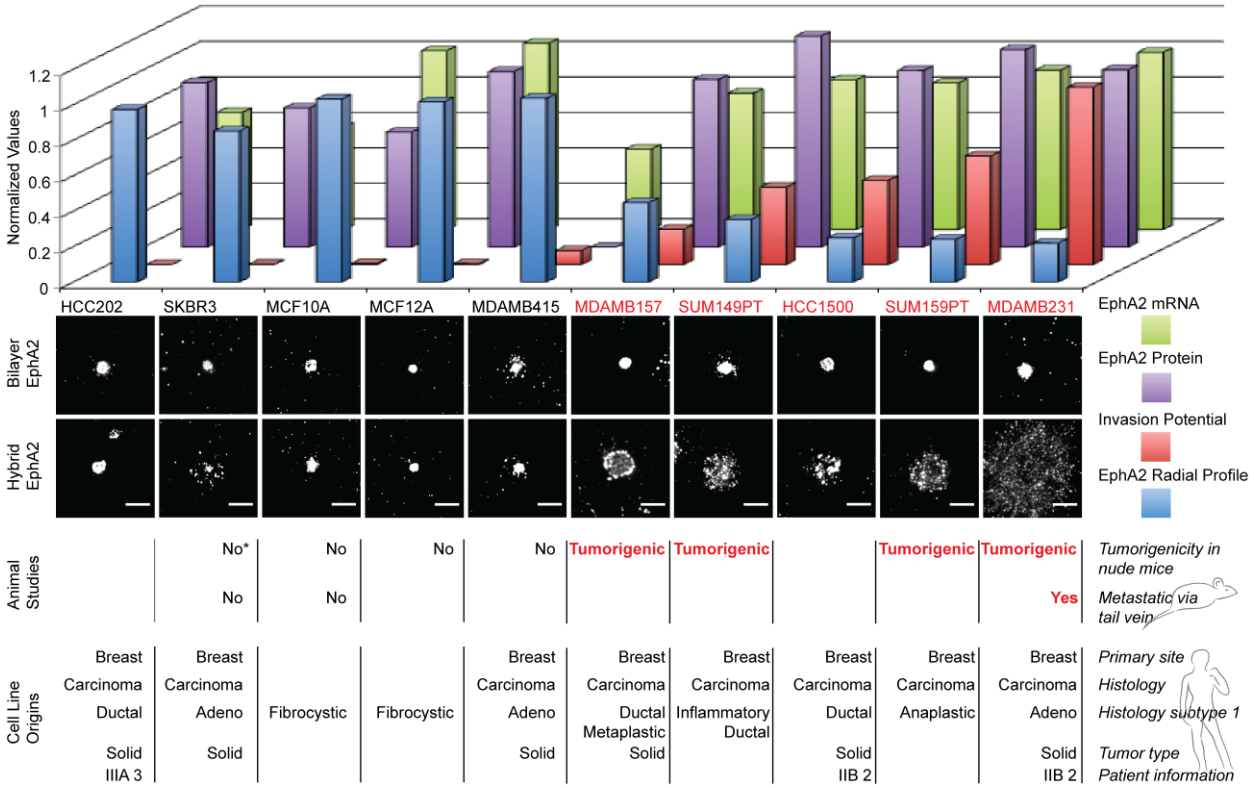

Fig. 5 Breast cancer cell line panel study. A panel consisting of 10 human breast cell lines are individually deposited on the hybrid platform. The radial profile of EphA2 was measured for cells that were deposited on the hybrid side and normalized to the radial profile of control cells from the same experiment, on the bilayer only side, to eliminate contributions from staining differences and cell-to-cell variations in EphA2 expression. For all cell lines, on the glass side displaying only mobile EA1, EphA2 is centrally transported. This is consistent with previous report.[20] For the cell lines on the nanoparticle side displaying the hybrid presentation, this situation changes dramatically, instead of forming a central domain, EphA2 clusters are distributed over the cell – substrate contact area as the respective invasion potential values increase. Invasion potential values, EphA2 protein expression levels, EphA2 mRNA levels, and cell line origins were taken from published sources.[19, 28, 34] The animal studies of tumorigenicity and metastasis, correlates with the EphA2 radial profile and invasion potentials, and were taken from published sources.[35-42] The cell line SKBR3 was found to be tumorigenic in one report (*).[43] A total of 200 cells were selected and analyzed. Scale bar are all 10 microns.

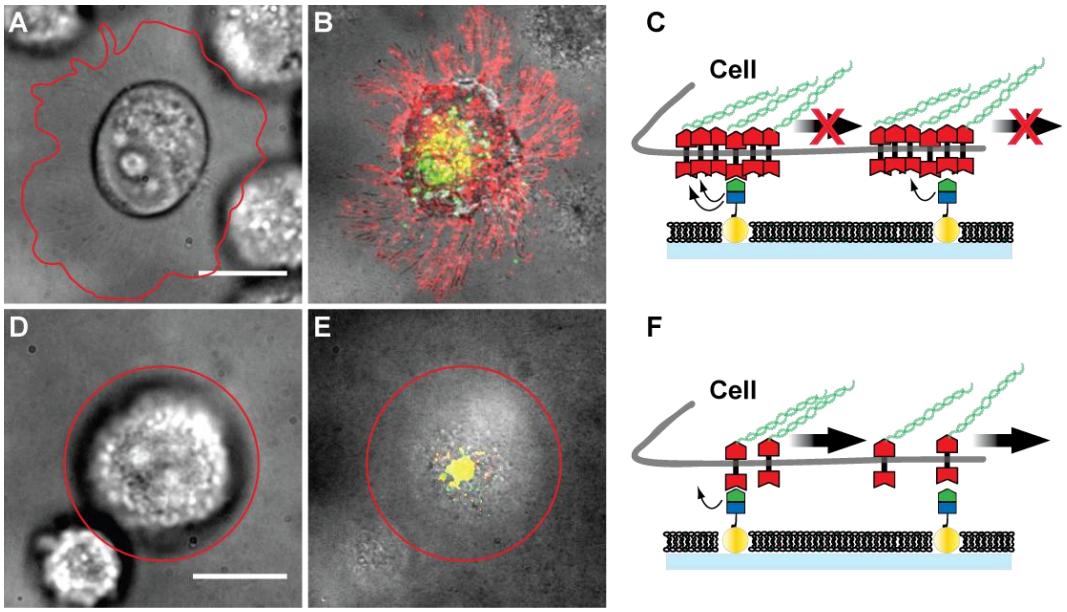

Fig. 6 Influence of EphA2 cluster formation on cell attachment revealed by the hybrid mobile/immobile presentation of ephrin-A1. **A) – C)** Pre-clustered EphA2 on the surface of invasive cell lines are restrained by molecules of immobilized EA1 linked to the nanoparticles. If one EphA2 receptor within the cluster unbinds from EA1, another one in the cluster can re-bind, and thus prevent radial transport. EphA2 clusters (red) are distributed along the cell protrusions imaged in RICM. Only a few EA1 clusters (green) are transported to the center of the cell-SLB contact area, and are co-localized with EphA2 (yellow). Cell outlines are highlighted by the red line. **D) – F)** For non-invasive cells, EphA2 is not pre-clustered and therefore individual EphA2 receptors can bind immobile EA1 ligands. As the cell applies a pulling force, these receptors can unbind and become centrally transported by re-binding to mobile EA1. Scale bars are 10 microns.

REFERENCES

1. Sporn, M.B. The war on cancer. *Lancet* **347**, 1377-1381 (1996).
2. Hanahan, D. & Weinberg, R.A. The hallmarks of cancer. *Cell* **100**, 57-70 (2000).
3. Vogel, V. & Sheetz, M. Local force and geometry sensing regulate cell functions. *Nat Rev Mol Cell Biol* **7**, 265-275 (2006).
4. Paszek, M.J. et al. Tensional homeostasis and the malignant phenotype. *Cancer Cell* **8**, 241-254 (2005).
5. Gschwind, A., Fischer, O.M. & Ullrich, A. The discovery of receptor tyrosine kinases: targets for cancer therapy. *Nat Rev Cancer* **4**, 361-370 (2004).
6. Lewis Phillips, G.D. et al. Targeting HER2-positive breast cancer with trastuzumab-DM1, an antibody-cytotoxic drug conjugate. *Cancer Res* **68**, 9280-9290 (2008).
7. Ciardiello, F. & Tortora, G. EGFR antagonists in cancer treatment. *N Engl J Med* **358**, 1160-1174 (2008).
8. Pasquale, E.B. Eph receptor signalling casts a wide net on cell behaviour. *Nat Rev Mol Cell Biol* **6**, 462-475 (2005).
9. Wimmer-Kleikamp, S.H. & Lackmann, M. Eph-modulated cell morphology, adhesion and motility in carcinogenesis. *IUBMB Life* **57**, 421-431 (2005).
10. Holland, S.J., Peles, E., Pawson, T. & Schlessinger, J. Cell-contact-dependent signalling in axon growth and guidance: Eph receptor tyrosine kinases and receptor protein tyrosine phosphatase beta. *Curr Opin Neurobiol* **8**, 117-127 (1998).
11. Keung, A.J., Kumar, S. & Schaffer, D.V. Presentation counts: microenvironmental regulation of stem cells by biophysical and material cues. *Annu Rev Cell Dev Biol* **26**, 533-556.
12. Dodelet, V.C. & Pasquale, E.B. Eph receptors and ephrin ligands: embryogenesis to tumorigenesis. *Oncogene* **19**, 5614-5619 (2000).
13. Pasquale, E.B. Eph receptors and ephrins in cancer: bidirectional signalling and beyond. *Nat Rev Cancer* **10**, 165-180 (2010).
14. Duxbury, M.S., Ito, H., Zinner, M.J., Ashley, S.W. & Whang, E.E. EphA2: a determinant of malignant cellular behavior and a potential therapeutic target in pancreatic adenocarcinoma. *Oncogene* **23**, 1448-1456 (2004).
15. Himanen, J.P. et al. Architecture of Eph receptor clusters. *Proc Natl Acad Sci U S A* **107**, 10860-10865.
16. Mudali, S.V. et al. Patterns of EphA2 protein expression in primary and metastatic pancreatic carcinoma and correlation with genetic status. *Clin Exp Metastasis* **23**, 357-365 (2006).
17. Jackson, D. et al. A human antibody-drug conjugate targeting EphA2 inhibits tumor growth in vivo. *Cancer Res* **68**, 9367-9374 (2008).
18. Hammond, S.A. et al. Selective targeting and potent control of tumor growth using an EphA2/CD3-Bispecific single-chain antibody construct. *Cancer Res* **67**, 3927-3935 (2007).
19. Salaita, K. et al. Restriction of receptor movement alters cellular response: physical force sensing by EphA2. *Science* **327**, 1380--1385 (2010).
20. Xu, Q., Lin, W.-C., Petit, R.S. & Groves, J.T. EphA2 Receptor Activation by Monomeric Ephrin-A1 On Supported Membranes. *Biophys J* (2011).
21. Lohmuller, T. et al. Supported Membranes Embedded with Fixed Arrays of Gold Nanoparticles. *Nano Lett*.

22. Nye, J.A. & Groves, J.T. Kinetic control of histidine-tagged protein surface density on supported lipid bilayers. *Langmuir* **24**, 4145-4149 (2008).
23. Lomüller, T. et al. Nanopatterning by block copolymer micelle nanolithography and bioinspired applications. *Biointerphases* **6** (2011).
24. Galush, W.J., Nye, J.A. & Groves, J.T. Quantitative fluorescence microscopy using supported lipid bilayer standards. *Biophys J* **95**, 2512-2519 (2008).
25. Groves, J.T., Ulman, N. & Boxer, S.G. Micropatterning fluid lipid bilayers on solid supports. *Science* **275**, 651-653 (1997).
26. Lin, W.-C., Yu, C.-H., Triffo, S. & Groves, J.T. Supported Membrane Formation, Characterization, Functionalization, and Patterning for Application in Biological Science and Technology. *Current Protocols In Chemical Biology*, 235-269 (2010).
27. McKinney, S.A., Murphy, C.S., Hazelwood, K.L., Davidson, M.W. & Looger, L.L. A bright and photostable photoconvertible fluorescent protein. *Nat Methods* **6**, 131-133 (2009).
28. Neve, R.M. et al. A collection of breast cancer cell lines for the study of functionally distinct cancer subtypes. *Cancer Cell* **10**, 515-527 (2006).
29. Janes, P.W. et al. Adam meets Eph: an ADAM substrate recognition module acts as a molecular switch for ephrin cleavage in trans. *Cell* **123**, 291-304 (2005).
30. Burridge, K. & Connell, L. A new protein of adhesion plaques and ruffling membranes. *J Cell Biol* **97**, 359-367 (1983).
31. Seiradake, E., Harlos, K., Sutton, G., Aricescu, A.R. & Jones, E.Y. An extracellular steric seeding mechanism for Eph-ephrin signaling platform assembly. *Nat Struct Mol Biol* **17**, 398-402.
32. Lackmann, M. et al. Distinct subdomains of the EphA3 receptor mediate ligand binding and receptor dimerization. *J Biol Chem* **273**, 20228-20237 (1998).
33. Hood, J.D. & Cheresh, D.A. Role of integrins in cell invasion and migration. *Nat Rev Cancer* **2**, 91-100 (2002).
34. Macrae, M. et al. A conditional feedback loop regulates Ras activity through EphA2. *Cancer Cell* **8**, 111-118 (2005).
35. Moyano, J.V. et al. AlphaB-crystallin is a novel oncoprotein that predicts poor clinical outcome in breast cancer. *J Clin Invest* **116**, 261-270 (2006).
36. Zhang, Y. et al. c-Jun, a crucial molecule in metastasis of breast cancer and potential target for biotherapy. *Oncol Rep* **18**, 1207-1212 (2007).
37. Mao, J.H. et al. FBXW7 targets mTOR for degradation and cooperates with PTEN in tumor suppression. *Science* **321**, 1499-1502 (2008).
38. Lehmann, B.D. et al. Identification of human triple-negative breast cancer subtypes and preclinical models for selection of targeted therapies. *J Clin Invest* **121**, 2750-2767.
39. Coletta, R.D. et al. Six1 overexpression in mammary cells induces genomic instability and is sufficient for malignant transformation. *Cancer Res* **68**, 2204-2213 (2008).
40. Xie, D. et al. Breast cancer. Cyr61 is overexpressed, estrogen-inducible, and associated with more advanced disease. *J Biol Chem* **276**, 14187-14194 (2001).
41. Liang, Z. et al. Silencing of CXCR4 blocks breast cancer metastasis. *Cancer Res* **65**, 967-971 (2005).
42. Hoenerhoff, M.J. et al. BMI1 cooperates with H-RAS to induce an aggressive breast cancer phenotype with brain metastases. *Oncogene* **28**, 3022-3032 (2009).

43. Fogh, J., Fogh, J.M. & Orfeo, T. One hundred and twenty-seven cultured human tumor cell lines producing tumors in nude mice. *J Natl Cancer Inst* **59**, 221-226 (1977).